SYNTHESIS AND CHARACTERIZATION OF MgB_2 SUPERCONDUCTING WIRES

A Thesis Submitted to
the Graduate School of Engineering and Sciences of
İzmir Institute of Technology
in Partial Fulfillment of the Requirements for the Degree of

MASTER OF SCIENCE

in Chemistry

by
Nesrin HORZUM

July 2008

İZMİR

We approve the thesis of **Nesrin HORZUM**

Prof. Dr. Tamerkan ÖZGEN
Supervisor

Assoc. Prof. Dr. Salih OKUR
Committee Member

Assoc. Prof. Dr. Durmuş ÖZDEMİR
Committee Member

9 July 2008

Date

Prof.Dr. Hürriyet POLAT
Head of the Department of Chemistry

Prof. Dr. Hasan BÖKE
Dean of the Graduate School of Engineering and Sciences

ACKNOWLEDGEMENTS

I would like to express my most sincere appreciate and gratitude to my dear supervisor Prof. Dr. İ. Tamerkan ÖZGEN for his supervision, help, support and encouragement he provided throughout my thesis.

I wish to express my gratitude to Assoc. Prof. Dr. Salih OKUR for giving me the opportunity to work with him and also I would like to thank him for his valuable comments and excellent suggestions patience in every step of my study.

I am pleased to pay my thanks to Technological Research Council of Turkey (TÜBİTAK) for funding the project (105M368) and providing the instruments and chemicals. Special thanks to Orhan ATİKER for supplying Boronsan boron powder for this project.

I would also thank to other member of the thesis committee, Assoc. Prof. Dr. Durmuş ÖZDEMİR for his recommendation and insightful comments.

Other thanks are owed to my dear friend Burcu ÜNSAL for her moral support, invaluable friendship and help in all my studies as well as to my friend Yelda DEMİRSAR who brought out good ideas in me.

I wish to acknowledge my colleagues in Department of Chemistry and Physics in İYTE for their friendship.

I am also very pleased to Evrim YAKUT and Gökhan ERDOĞAN at Material Research Center for their kind help in performing the XRD and SEM-EDX analysis. I would also thank to Mücahit SÜTÇÜ for his help in performing the OM analysis.

Also, I am very grateful to Serkan POLAT for being the best ever friend for me. He has been a true and great supporter and he has endless love to me through both my good and bad times during this thesis studies.

Finally, I would especially like to send my deep gratitude and appreciation to I am thankful to my dear parents Güler-Hüseyin HORZUM and my brother Uğur HORZUM for their unconditional love, understanding and endless support during all through my life.

ABSTRACT

SYNTHESIS AND CHARACTERIZATION OF MgB_2 SUPERCONDUCTING WIRES

In this study, the superconducting properties of laboratory synthesized MgB_2 was investigated. In the first part, MgB_2 synthesis using commercial magnesium and boron (95-97% purity), and its microstructural and electrical characterization was investigated. Effects of sheath material and annealing temperatures were also examined. The microstructural studies showed that when Cu tubes were used as sheath material, $MgCu_2$ forms instead of MgB_2 even at 700°C, while on Fe clad cores, the major phase was MgB_2 with minor MgO constituent. The transition temperatures of Fe clad wires were measured between 39K and 40K, whereas no transition temperature was observed for Cu clad wires. The I_c value of the Fe clad MgB_2 wire was about 25 A at 4K, while the copper clad wire could not carry current and formed resistance. In Fe clad wires, better results were obtained at annealing temperature of 800°C for 30 minutes.

In the second part, MgB_2 synthesis using commercial magnesium and boron (90% purity) was tried. 0-5-10-15 wt% of Mg doping and, additionally annealing temperatures were examined. Powder-In-Tube method was used for wire production. 10 wt% Mg addition was seen to be beneficial as compared to the stoichiometric MgB_2. 750°C was found to be the most suitable temperature for the formation of MgB_2 phase. The I_c value of the wire was measured as 13 A at 4K and it showed a broader transition with non-zero resistivity, transition temperature of 24K.

In the third part, 200 m long four filament MgB_2/Cu wire was successfully produced in laboratory conditions.

ÖZET

SÜPERİLETKEN MgB_2 TELLERİN SENTEZİ VE KARAKTERİZASYONU

Bu çalışmada, laboratuvarda sentezlenen magnezyum diborürün süperiletken özellikleri incelenmiştir. Çalışmanın ilk bölümünde, ticari magnezyum ve bor (95-97% saflıkta) kullanılarak MgB_2 sentezlenmiş, ve mikroyapısal ve elektriksel tanımlanması yapılmıştır. Kılıf maddesinin etkileri ve tavlama sıcaklıkları da incelenmiştir. Mikroyapısal incelemeler, kılıf olarak bakır borular kullanıldığında 700^oC sıcaklıkta bile MgB_2 yerine $MgCu_2$ oluştuğunu, ancak demir boru kılıflar kullanıldığında tel içinde oluşan ana maddenin MgB_2 olduğunu ve az miktarda MgO içerdiğini göstermiştir. Demir kılıflı tellerde geçiş sıcaklığı 39K ve 40K arasında ölçülürken, Cu kılıflı tellerde bir geçiş sıcaklığı ölçülememiştir. Ayrıca, Fe kılıflı MgB_2 tellerin I_c değeri 4 K de 25 A olarak ölçülmüş, buna karşılık Cu kılıflı teller akım taşıyamamış ve bir direnç oluşturmuştur. Fe kılıflı tellerde, 800°C sıcaklıkta 30 dakika tavlamayla daha iyi sonuçlar alınmıştır.

Çalışmamızın ikinci bölümünde ticari magnezyum ve bor (90% saflıkta) kullanılarak MgB_2 sentezi denenmiştir. Ağırlıkça % 0-5-10-15 Mg katkılama ve buna ek olarak tavlama sıcaklıkları incelenmiştir. MgB_2 tel üretimi için Tüp İçinde Toz (TİT) yöntemi kullanılmıştır. %10 ağırlıkta fazla Mg eklenmesinin, stokiyometrik MgB_2'e göre daha iyi sonuçlar verdiği gözlenmiştir. MgB_2 fazının oluşumunda en uygun ısıtma sıcaklığının 750°C olduğu bulunmuştur. Telin I_c değeri 4 K de 25 A olarak ölçülmüş ve 24 K geçiş sıcaklığında sıfır olmayan bir dirençle daha geniş bir geçiş gözlenmiştir.

Çalışmamızın üçüncü bölümünde, 200 m uzunluğunda içinde dört filamanlı MgB_2/Cu teli laboratuar şartlarında başarıyla üretilmiştir.

Dedicated to;

the memory of my grandfather

and

my lovely family for being with me in all my life...

TABLE OF CONTENTS

LIST OF FIGURES

LIST OF TABLES

CHAPTER 1

INTRODUCTION

1.1. The Element Boron

Although boron compounds and especially borax have been known for centuries, the elemental boron was first obtained in 1808 by the French chemist Joseph Gay-Lussac and Baron Louis Thenard and the English chemist Sir Humphry Davy by heating boroxide with potassium. Davy named this element as *boron* which was obtained from **BOR**ax and which resembled carb**ON**. In 1892, H. Moisson reduced boron oxide with magnesium and obtained elemental boron with 86% purity. Boron obtained by this method was named Moisson's Boron. In 1909, W. Weintraub, succeeded in obtaining boron of 99% purity by the thermal decomposition of BCl_3 (Baudis and Fichte 2002).

The element boron which takes place in the 2nd period and Group III A of periodic table consists of two stable isotopes with mass numbers 10 and 11 and atomic number 5. Its chemical symbol is **B,** and it is the only element which has the characteristic of being between metal and nonmetal semiconductor in group III A. Boron is never found as a free element in nature, but is found as inorganic borates due to its high affinity to oxygen. Boron is commonly found in soil, rocks and water on the earth's surface. The boron content in soils is generally 10-20 ppm. It is found in high concentrations in the western regions of USA and the region lying between the Mediterranean and Kazakhstan. In sea water it ranges between 0.5-9.6 ppm, and in fresh water from 0.01-1.5 ppm (Sivrikaya and Saraçbaşı 2004).

The different characteristics of the compounds formed with metal or nonmetal elements provide opportunities to use many boron compounds in industry. Boron acts as a nonmetal in its compounds but it differs due to its being an electric conductor such as pure boron or carbon. Crystallized boron resembles diamond in appearance and optical characteristics, and is nearly as hard as diamond too.

1.1.1. The Structure of Boron

Boron has various allotropic forms such as amorphous and crystalline polymorphic. Crystalline boron has some different allotropic forms, the best known are α-rhombohedral boron and β-rhombohedral boron. Apart from these it has four more tetragonal structures, but these can be stabilized by small amounts of nitrogen and carbon. (Baudis and Fichte 2002).

The structure of α-rhombohedral boron is the simplest allotropic structure, and is described as a slightly deformed cubic close packing of B_{12} icosahedra. Rhombohedral unit cell has lattice parameter of a_o= 5.057 Å, axial angle of a=58.06^o and includes 12 B atoms.

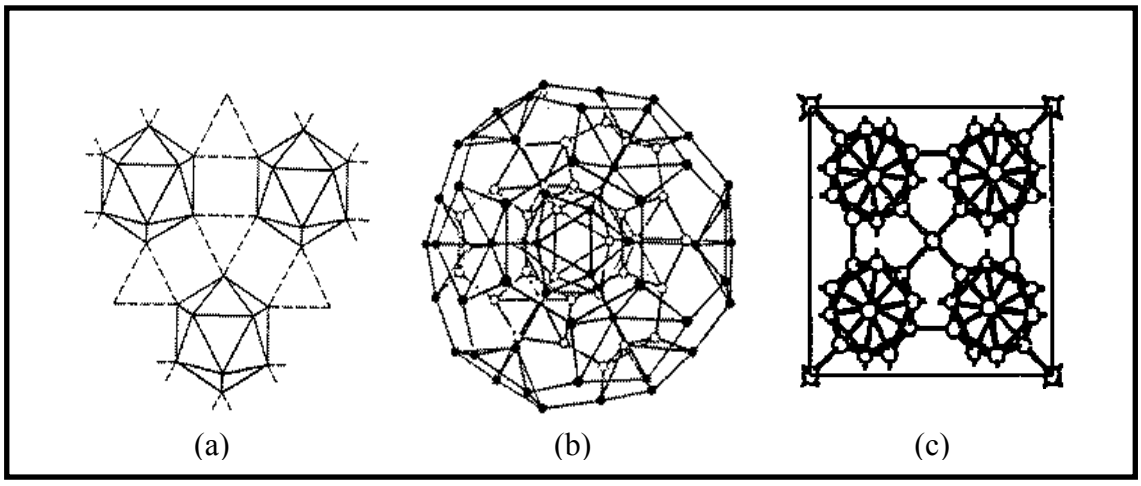

Figure 1.1. The Crystal Structures of Boron a) α-Rhombohedral Boron b) β-Rhombohedral Boron c) α-Tetragonal Boron (Source: University of Oxford 2007)

Thermodynamically, the most stable polymorph of boron is the beta-rhombohedral modification and with 105 B atoms in the unit cell, it is the most complex structure (a_o=10.145 Å, a=65.28^o). The B atoms in unit cells form an outer shell resembling C_{60} (University of Oxford 2007).

The first made crystalline polymorph B was named as α--tetragonal boron and it was found that it contained 50 boron atoms in the unit cell ($4B_{12}$+2B) (Baykal 2003). The final researches show that this phase cannot form in the absence of nitrogen and carbon and, depending on the preparation conditions, has the formulas of $B_{50}C_2$ or $B_{50}N_2$.

1.1.2. Physical Characteristics

The physical characteristics of elemental boron are greatly affected by the crystal structure and purity. With the density of 2.30 g/mL, the amorphous boron's melting point is 2300°C, sublimation point is 2550°C, α-rhombohedral boron melts at 2180°C, sublimates at 3650°C and its density is 2.46 g/mL. (Mark and McKetta 2001).

Table 1.1. Physical Characteristics of Boron
(Source: Evcin 2007, Greenwood 1973, Mark and McKetta 2001)

Atomic Number	5	
Atomic Weight	10.811 g/mol	
Atomic Radius	1.17Å	
Melting Point	2300°C	Amorphous
	2180°C	α-rhombohedral
Boiling Point	3660°C	
Sublimation Point	2550°C	Amorphous
	3650°C	α-rhombohedral
Density (at 20°C)	2.30 g/mL	Amorphous
	2.35 g/mL	β-rhombohedral
	2.46 g/mL	α-rhombohedral
Molar Volume	4.68 cm^3/mol	
Hardness	2390 kg/mm^2	Knoop
	9.3	Mohs
	49000 MPa	Vickers
Conductivity	1.0 $e^{-12}10^6$/cm	Electrical
	0.274 W/cmK	Thermal
Heat Capacity (at 27°C)	12.054 JK^{-1} mol^{-1}	Amorphous
	11.166 JK^{-1} mol^{-1}	β-rhombohedral
Entropy (25°C)	6.548 JK^{-1} mol^{-1}	Amorphous
	5.875 JK^{-1} mol^{-1}	β-rhombohedral
Enthalpy of Atomization (at 25°C)	573.2 kj/mol	
Enthalpy of Fusion	22.18 kj/mol	
Enthalpy of Vaporization	480 kj/mol	
Heat of Vaporization	489.7 kj/mol	
Vapor Pressure (at 2300°C)	0.348 Pa	

Boron is the hardest element after diamond which is an allotrope of carbon. α-rhombohedral boron is a reddish brown, β-rhombohedral boron is a bright greyish black, its amorphous form is a brownish grey (Baudis and Fichte 2002). At room temperature elemental boron is a poor electrical conductor but is a good electrical conductor at high temperatures.

1.1.3. Chemical Characteristics

The chemical characteristics of the element boron depend on the morphology and the magnitude of its particles. The amorphous boron at micron size goes into reaction easily and intensively while crystalline boron does not react easily.

Crystalline boron, which is chemically nonmetal, does not react with water, air, hydrochloric/hydrofluoric acids in normal conditions; it can only transform into boric acid with high concentrated nitric acid in heated ambient.

Table 1.2. Chemical Characteristics of Boron
(Source: Evcin 2007)

Standard electrode potential	$B + 3H_2O \rightarrow H_3BO_3 + 3H^+ + 3e^-$	- 0.73 V
Electron affinity	32 kj/mol – 0.332 eV	
Electronegativity	2.04 (Pauling)	
	2.01 (Mulliken)	
Ionic Radius	0.25 nm	
Atomic Radius	0.80-0.95 nm (depending on the type of bonding)	
First ionization energy	798 kj/mol – 8.27 eV	
Second ionization energy	2426 kj/mol – 25.15 eV	
Third ionization energy	3658 kj/mol –37.92 eV	

The electronic configuration of boron is $1s^2\ 2s^2\ 2p^1$, dictates predominant trivalency. However, simple B^{3+} ions do not exist. Because boron's bonding orbital are more than its electrons (4 orbitals, 3 electrons), it behaves as an electron pair acceptor, a Lewis acid, and has a tendency to form multicentered bonds. In high temperatures, by reacting with oxygen it forms boron oxide (B_2O_3), and under the same circumstances forms compounds used in industry such as boron nitride (BN) with nitrogen, titanium boride with titanium (TiB_2). It does not react directly with hydrogen, but forms

borohydrides indirectly. It forms boron trihalides by intensively reacting with halogens (F_2,Cl_2,Br_2). At room temperature, boron (III) fluoride is obtained by fluoride, and with chloride, boron (III) chloride is obtained at 500°C and with bromide, boron (III) bromide is obtained at 600°C (Cueilleron 1944).

Elemental boron is an effective reducing agent, while reducing water vapor to hydrogen (800°C), nitrogen oxide to boron nitride; itself is oxidized to boron oxide (Cueilleron and Thevenot 1977). When transition metal oxides such as Fe_2O_3, TiO_2 and Cr_2O_3 react with elemental boron, boron oxide and metal borides are formed.

While boron does not react with NaOH solution, it totally reacts with molten sodium carbonate, Na_2CO_3 or molten sodium carbonate-sodium nitrate mixture.

1.2. Boron Products

By considering the production stages and processes, boron minerals and commercial products that are obtained and find usage area in the world and Turkey today can be divided into three groups: raw boron products, refined boron products and specialty boron products.

1.2.1. Raw Boron Products

Raw boron products found as concentrated boron ore in nature. The primary boron minerals having commercial importance are shown in Table 1.3. 90% of raw boron products are used in the production of refined boron products such as boric acid, borax penthahydrate and borax decahydrate.

1.2.2. Refined Boron Products

These are products that are obtained by using the appropriate raw boron ore with or without chemical reaction to remove away substances apart from the main mineral. Refined boron products are the most consumed derivatives of boron. These products may be used in the production of special boron products as a source of boron on economic bases. Refined boron products and amounts of boron oxide produced in the world at a commercial dimension are shown in Table 1.4.

Table 1.3. Raw Boron Products
(Source: National Boron Research Institute 2008)

Kernite	$Na_2B_4O_7.4H_2O$	Pandermite	$Ca_4B_{10}O_{19}.7H_2O$
Tincalconite	$Na_2B_4O_7.5H_2O$	İnderit	$Mg_2B_6O_{11}.15H_2O$
Tincal	$Na_2B_4O_7.10H_2O$	Szaibelyite	$MgBO_2(OH)$
Probertite	$NaCaB_5O_9.5H_2O$	Hydroboracid	$CaMgB_6O_{11}.6H_2O$
Ulexite	$NaCaB_5O_9.8H_2O$	Boracid	$Mg_3B_7O_{13}Cl$
Colemanite	$Ca_2B_6O_{11}.5H_2O$	Asharite	$Mg_2B_2O_5.H_2O$
Meyerhofferit	$Ca_2B_6O_{11}.7H_2O$	Datolite	$Ca_2B_2Si_2O_9.H_2O$
İnyoit	$Ca_2B_6O_{11}.13H_2O$	Sassolite (boric acid)	H_3BO_3

Table 1.4. Refined Boron Products
(Source: National Boron Research Institute 2008)

Name of Product	Formula	B_2O_3 (%)
Boron oxide (anhydrous boric acid)	B_2O_3	100,0
Sodium oxiborate	$Na_2B_8O_{13}$	81,8
Anhydrous borax	$Na_2B_4O_7$	69,3
Sodium metaborate	$Na_2B_2O_4.4H_2O$	64,2
Boric acid	H_3BO_3	56,5
Borax pentahydrate	$Na_2B_4O_7.5H_2O$	47,8
Boraks decahydrate	$Na_2B_4O_7.10H_2O$	36,5
Sodium perborate	$NaBO_3.4H_2O$	22,0

1.2.3. Specialty Boron Chemicals

Specialty boron chemicals are products used for a specific aim produced from raw and refined boron products by advanced technological methods.

Table 1.5. Specialty Boron Chemicals
(Source: Sümer 2004)

Elemental Boron
Inorganic Borates
Boron Halides
Fluoroboric Acids and Fluoroborates
Refractory Boron Compounds ✓ Boron Carbide ✓ Boron Nitride ✓ Metal Borides
Ferroboron and other Boron Alloys
Borohydrides
Boric acid esters
Boranes

Our 1.2 billion dollar share in the world boron market owning approximately 65% of world reserves remains at a level of 20% with our 1.2 million ton tuvenane ore production. When examined from the viewpoint of special boron chemicals, we cannot even achieve 1%. These rates are evidence of our inability to benefit effectively from this important raw material resource. The most important reason for this is that there are not necessary investments made in refined or specialty boron chemicals which create more value added.

1.3. Industrial Application Areas of Boron Products

Boron minerals and compounds are used in various branches of industry and in the manufacture of different materials and products, from the glass industry to communication devices and from the car industry to the agriculture sector.

Boric acid and borax are used in producing special glasses which require features such as surface hardness, being both heatproof and endurable. Also borax and boric acid are used in increasing flow of enamel in the ceramics industry and fiber glass which provides insulation, and in decreasing their density and degree of saturation temperature.

Elemental boron nowadays is used in military activities such as illumination, nuclear weapons and as maintenance in nuclear power reactors.

Sodium perborate from inorganic borates is used in detergents, bleaches and textiles, ***sodium metaborate*** is used in adhesives, detergents, pesticides, photography and textile, ***sodium pentaborate*** is used in fertilizers and fire retardants. ***Potassium pentaborate*** is used for stainless steel and in welding and soldering processes in non-iron metals; ***barium metaborate*** is used as corrosion preventer; ***ammonium diborate*** is used in urea-formaldehyde resins for the purpose of neutralization, ***ammonium pentaborate*** is used as an electrolyte in electrolytic capacitors. ***Calcium borate*** is used in antifreeze compounds, metallurgic fluxes and porcelain production, and ***copper borate*** is used for preventing fungus formation (Smith 2002).

The most commonly used boron halides is ***boron trifloride*** and it plays an important role in organic synthesis reactions. It functions as a catalyst in Friedel-Crafts alkylation reaction, esterification reactions and in the sulfonation and nitration of aromatic compounds. Boron trifloride is used as a precursor in most olefin polymerization reactions and also used in alkanes and alkenes isomerization. Another boron halides, ***boron trichloride***'s most important praxis is its usage in preparing boron fibers. When greatly heated tungsten filament is passed through a system consisting of boron trichloride and hydrogen, strong boron fibers are formed by boron trichloride being reduced to boron. As boron trichloride is a strong Lewis acid as boron trifloride, it is used as a catalyst in organic reactions. A close resemblant ***boron tribromide*** functions as an precursor in olefin polymerizations. There is no known commercial implementation of boron triiodide (Brotherton and Weber 2002).

Fluoroboric acid is used in preparing other fluoroborate salts and also as a dipping solution for electroplating and aluminum surface operations. Molten alkali-metals and ammonium fluoroborates are good solvents for metal oxides used for military purposes. A mixture of LiF and $NaBF_4$ is used as a cooling agent in nuclear reactors and as a solvent for materials that may undergo fission. Alkali metal fluoroborates and fluoroboric acid catalyzes organic synthesis and polymerization reactions. ***Lithium fluoroborate*** is used as an electrolyte in lithium-sulphur batteries.

Boron carbide is the most commonly used among specialty boron chemicals. With its neutron absorption ability and being heatproof, it is used in armoring military vehicles and in nuclear reactors. Metal matrix composites are made out of boron carbide and aluminum or aluminum alloys.

Boron nitride, hot pressed boron nitride, is less fragile than many ceramic materials. It is mechanically hard, and is used in drilling and cutting. Powdered hexagonal boron nitride is used in a large area as a greasing material in high temperatures.

Ferroboron with its usage as alloying steel with boron and as a amorphous material in transformer nucleus forms an important usage area. Boron-Nickel alloys and Boron-Cobalt alloys are used in high frequency transformer nucleus. Wires produced from these alloys are preferred to be used in the production of saddle in equipments such as EKG (Kılıç 2004).

Borohydrides are used as a reduction material to obtain hydrogen. Free oxygen released by decomposition of sodium borohydride with water, which can be used in fuel batteries and in internal combustion engines as a clean fuel (Kar, et al. 2006).

Methyl borate is the most important ***boric acid ester*** commercially, because they are used in the synthesis of sodium borohydrides and diboranes. Methyl borate azeotropes are used especially in Europe as a material that reduces the melting point of welds. Borate esters are used as flame retardants, oxidation of hydrocarbons, in the preparing of trialkylboranes and as lubricating material.

Boranes are very reactive and require great care. Diboran is a strong but selective reducer in organic chemistry. It is an electrophilic reactive and reacts with nucleophilic alkali metal boron and aluminum hydrides.

Metal borides, Cr, Mo, Ti, Tn, Ni, Zr, Hf, and Ce, borides are used in rocket exhausts, turbine wings, heat conductor, electrical contact, and crucible production. ***Lanthanium hexaboride,*** LaB_6 has metallic characteristic and being durable

thermically and chemically, is used as a cathode material in electrolysis processes**.** ***Zirconium diboride***, ZrB_2 is extremely durable against heat changes and corrosion. For this reason it is used as a protective plate and crucible material in thermo elements. Zr and Ti borides or carbide compounds are preferred in coating cells in aluminum electrolysis (Çeçen 1969). **Magnesium Diboride,** MgB_2 which has superconductive characteristics, can be used in high power transformers, conducting wires carrying high voltages and most importantly in the magnetic coils in MRI equipments. Also, differing from other borides, magnesium boride is in a hydrolyzed form able to produce boron hydride compounds.

1.4. The History of Boron Mining and Importance for Turkey

In the history, the Babylonians were the first to import borax from the Far East and use it in gold mining. The first borax resources were obtained from Tibetan Lakes and after Marco Polo brought borax to Europe the modern boron industry started. In 1702, Hommerg heated borax with iron (II) sulphate and obtained boric acid in Italy (Çeçen 1969). The first commercial boric acid was produced in 1830. In 1864, the first commercial boron production was carried out in California and Turkey's boron deposits were run foreign companies for approximately a hundred years between 1865 and 1958. In 1935, Etibank and the General Directorate of Mineral Research and Exploration were founded in order to conduct the activities of Mine Prospecting and commissioning in Turkey. Turkey's first boron mine export was undertaken in 1959 by realizing the first mine ore production from the deposits of Emet, Kütahya Etibank. 15 years after Türk Boraks Madencilik A.Ş. and their Turkish partners finding the reserves of Kırka Sodium Borates in 1960, in 1975 the Bandırma Sodium Perborate facility was commissioned. Later in 1984 Kırka I. Boron derivatives facility, in 1987 the Bandırma II. Boric Acid facility, in 1996 Kırka II. Borax pentahydrate facility, in 2001 the Kırka III. Borax pentahydrate facility and lastly in 2004, the Emet Boric Acid facility started to be commissioned.

The most important boron reserves in the world lie in Turkey, Russia and the USA. When it is viewed from the viewpoint of reserves, Turkey's share in boron oxide is 64%. While the reserve span of Turkey's boron reserves is 389 years, the world second largest reserve country Russia's boron reserve has a life span of 69 years. When

the world boron reserves and increased rate of consumption of these reserves are viewed, in 50 to 80 years our country's boron reserves have a high possibility of being the sole source of boron. World boron reserves and resources are shown in Table 1.6.

Table 1.6. World Boron Reserves and Resources (thousand tons, as B_2O_3) (Source: Kılıç 2004)

Country	Proven Economic Reserve	Probable Possible Reserve	Total Reserve	Share in Total Reserve (%)	Life-span (Year)
Turkey	224,000	339,000	563,000	64	389
Russia	40,000	60,000	100,000	11	69
USA	40,000	40,000	80,000	9	55
Chili	8,000	33,000	41,000	5	28
China	27,000	9,000	36,000	4	25
Peru	4,000	18,000	22,000	2	15
Bolivya	4,000	15,000	19,000	2	13
Kazakhstan	14,000	1,000	15,000	2	10
Argentina	2,000	7,000	9,000	1	6
TOTAL	363,000	522,000	885,000	100	610

The known primary boron deposits in Turkey are situated in West Anatolia. Turkey's reserve is provided by Bigadiç with 37%, Emet by 34%, Kırka by 28%, and Kestelek Boron Facility by 1%. Turkey's boron reserves and facilities are shown in Table 1.7. (Kılıç 2004).

Table 1.7. Turkey's Boron Reserves and Facilities
(Source: Kılıç 2004)

Production Place	Mineral	Reserve (million tons)	% B_2O_3	Capacity (Ton/Year)	Production (Ton/Year)
Kırka Boron Facility	Tincal	605.5	25.8	200,000	558
Emet Boron Facility	Colemanite	835.6	27.5-28.5	500,000	300
Bigadiç Boron Facility	Ulexite	49.2	29.1	200,000	200
	Colemanite	576.4	29.4	200,000	90
Kestelek Boron Facility	Colemanite	7.7	25-33.2	100,000	60
TOTAL		2074.4		1,200,000	1208

1.5. Conductivity

Electrical conductivity involves a flow or current of free electrons that in the outer shells of atoms are bound more loosely to the nucleus. Conductivity is the reciprocal of electrical resistivity and has the SI units of siemens per meter ($S \cdot m^{-1}$).

Materials can be classified as insulators, semiconductors, conductors and superconductors according to their conductivities (The Institution of Electronics and Telecommunication Engineers 2008).

Insulators: Insulating materials such as wood, glass, plastic, rubber, silicon dioxide, and silicon nitride that resist the flow of electric current. Bulk resistivity is within the range of 10^{10} to 10^{22} ohm-centimeter to be considered an insulator. Insulators have tightly bound electrons in the valence shell that remain there even in the presence of high voltage electric fields (Microwave Encyclopedia 2006). The valence band of these substances is full while the conduction band is completely empty. The forbidden energy gap between valence band and conduction band is very large (8 eV) as shown in Figure. 1.2.a. Therefore, a big amount of energy; that is, a very high electric field is necessary to repel the valence electrons to the conduction band. This is the reason, why such material doesn't simply conduct in the ordinary situation and are designated as insulators.

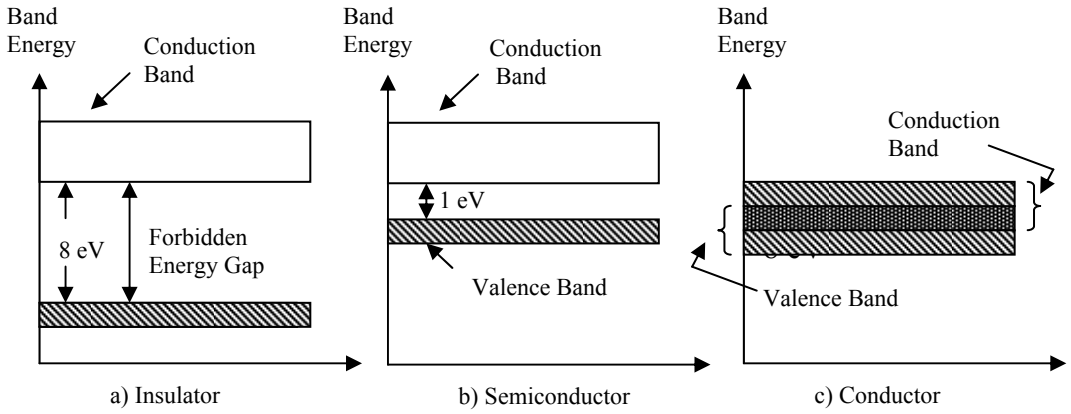

Figure 1.2. Energy Band Diagrams

(Source: The Institution of Electronics and Telecommunication Engineers 2008)

Semiconductors: Electrical conductivity of semiconductors like carbon, silicon, and germanium lies in between the conductors and insulators. They have bulk resistivity in the range of 10^{-4} ohm-cm to 10^{3} ohm-cm. Semiconductor materials have 4 electrons in their outer shell. When bonded together in a crystal lattice, atoms share electrons such that they each have eight electrons in the outer shell. Electrons are somewhat loosely bound so they can become carriers in the presence of an electric field (Microwave Encyclopedia 2006). The valence band of semiconductor materials is almost filled, but the conduction band is almost empty. The forbidden energy gap between valence and conduction band is very small (1 eV) as shown in Figure 1.2.b. Hence, relatively a smaller electric field is required to push the valence electrons to the conduction band. Even at room temperature, when some heat energy is given to the valence electrons, a few of them cross over to the conduction band giving minor conductivity to the semiconductors. As the temperature is increased, more valence electrons cross over to the conduction band and the conductivity of the material increases. Therefore; these materials have negative temperature co-efficient of resistance (Balkan and Erol 2005).

Conductors: Conductor materials such as copper, aluminum, silver which allow the passage of current through them have a bulk resistivity within the range of 10^{-6} to 10^{-4} ohm-cm. They have loosely bound electrons (one or two) in the valence shell that can move easily under the influence of a voltage to form current. The valence band of these conductor materials overlaps the conduction band as shown in Figure 1.2.c. Due to this overlapping, a large number of free electrons are available for conduction. This is the

reason, why a slight potential difference applied across them causes a heavy flow of current through them.

Superconductors: Superconducting materials have a bulk resistivity of zero. A superconductor loses all resistance to the flow of electric current when it is cooled below a certain temperature, called the critical temperature (Tc) or transition temperature. These materials suddenly achieve zero resistance below the transition temperature and gain other magnetic and electrical properties.

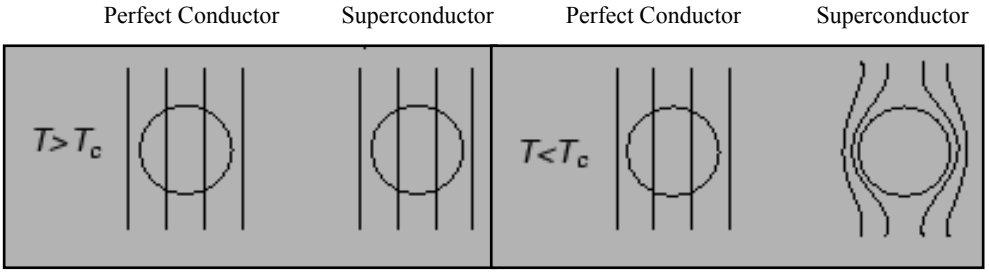

Figure 1.3. Comparison of a Perfect Conductor and a Superconductor
(Source: Helsinki University of Technology 2008)

The difference between a superconductor and a perfect conductor is that the superconductor materials expel all magnetic fields when it goes through the superconducting transition. In the superconducting state, magnetic flux vanishes inside the material in all circumstances because of the Meissner effect.

1.6. The Aim of the Study

The purpose of this study is to synthesize and characterize in-situ MgB_2 superconducting wires. The effects of precursor boron powder on Mg and this influence on the superconducting properties of MgB_2 was investigated. The importance of B for the MgB_2 production is clear, and this makes our study even more important since Turkey has the biggest boron sources in the world. In addition, the effects of sheath material, Mg doping and annealing temperatures were also examined. For this reason, iron and copper sheathed in-situ MgB_2 wires were produced by Powder In Tube (PIT) method. The microstructural and electrical characterization were done through XRD, SEM/EDX, OM, R-T and V-I measurements.

CHAPTER 2

SUPERCONDUCTIVITY

2.1. The Characteristics of Superconductors

Superconductors are matters that lose their resistance completely against electrical currents when their temperature is dropped to a critical temperature. The history of superconductivity started in 1908 when Heike Kamerlingh Onnes, a physicist from the Netherlands, was trying to liquefy helium which has a boiling point of 4.2 K. Onnes, in 1911 at the University of Leiden analyzed metals resistance at low temperatures, found out that electrical resistance of Hg went to zero at 4.2 K and defined it as a superconductor (Onnes 1911). After the discovery of superconductivity in 1911, it was observed that many metals resistances went to zero under a critical temperature (Tc), peculiar to each metal. Due to his works on liquid helium and the characterization of metals at low temperatures, he got the Nobel Physics Prize in 1913.

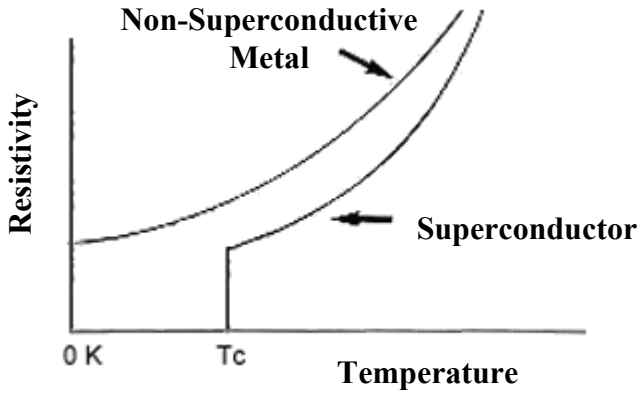

Figure 2.1. Critical Temperature Dependence of Resistivity of Non Superconductive and Superconductor Metal (Source: Wesche 1998)

In 1933, Walter Meissner and his student Robert Ochsenfeld analyzed the magnetic characteristics of superconductors and discovered that when a superconducting material makes the transition from normal state to superconducting state, it actively repels magnetic field (Meissner and Ochsenfeld 1933). The magnetic

field does not go through the internal of the superconducting material, that's why they show perfect diamagnetic properties. This is called the Meissner effect and was found to be an intrinsic property of superconductors.

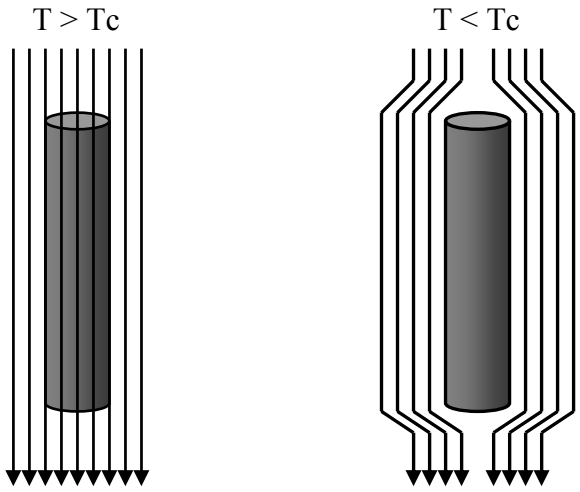

Figure 2.2. Meissner Effect
(Source: Harvard University 2008)

The critical temperature (Tc) of superconductors in a magnetic field decreases as the magnetic field increases. When the magnetic field exceeds a critical Hc point, the superconductivity is lost and it acts as a normal conductor.

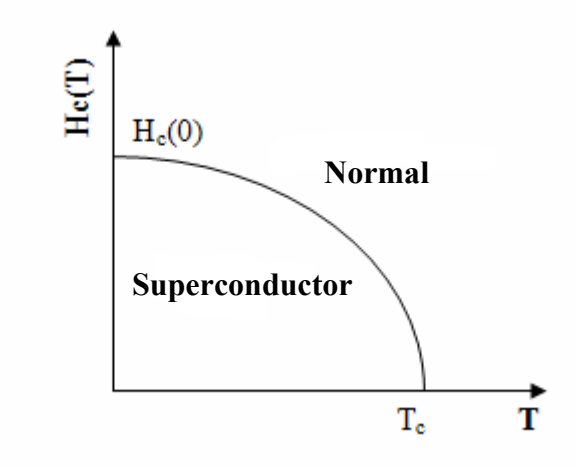

Figure 2.3. Schematic Representation of Critical Temperature Dependence of Critical Magnetic Field (Source: Wesche 1998)

It is found that critical magnetic field changes with respect to temperature as;

$$Hc\ (T) = H_c\ (0)\ [1- (\ T / T_c)^2]$$

Here, Hc(0) is the magnetic field to corrupt superconductivity at 0K. Tc is the transition temperature from normal state to superconducting state (Bardeen, et al. 1957).

In 1935, Fritz and Heinz London brothers improved superconductivity as the theory of electrodynamics. According to the London equation, when going inwards the superconductive surface, the magnetic field decreases exponentially. (London and London 1935). So, the magnetic field compatible with the Meissner effect, becomes zero in the sample. The magnetic field resulting from surface currents penetrates to a certain degree and the characteristic decay length of this formation is determined as London penetration depth (λ).

V. Ginzburg and L. Landau put forward a theoretical explanation on superconductors based on general symmetrical characteristics. (Ginzburg and Landau 1950). Although the *Ginzburg – Landau theory* explains the macroscopic characteristics of superconductors, it is insufficient in explaining microscopic characteristics.

The first theory based on understanding superconductivity was developed by three physicists from the University of Illinois in 1957; John Bardeen, Leon Cooper and Robert Shcrieffer (Bardeen, et al. 1957). This approach known as BCS, explains how electrons flow in regularity, locked to each other in a vibrating lattice structure. Free conductive electrons in normal metals, form a resistance because their movements are restrained by events such as friction and collision while moving under electric fields among positive ions inside crystal structures. When an electron is passing near an ion, it pulls the ion towards itself, but after a short while it goes back to its former position resembling an arc system. If the crystal structure is cooled under a certain transition temperature, it takes time to go back to its former position. While a second electron goes after the former, its movement gains speed by being pulled by this ion. So, the crystal potential that forms as a result of the deformation of the first electron provides an attraction field for the second electron. This can be thought as two electrons pulling each other indirectly. Electrons that are coupled like this are called the Cooper couple and they play an important role in forming superconductivity.

Alexei Alekseevich Abrikosov analyzed the characteristics of superconductors in the presence of external magnetic fields. In 1957, he found that superconducting materials divide into two as Type I and Type II. (Abrikosov 1957). In Type I superconductors, magnetization increases until it reaches the critical magnetic field and drops to zero at that point, meaning it acts as a normal superconductor. These types of superconductors are soft, diamagnetic, and are superconductor in low temperatures. Among these, pure metallic materials such as Al, Hg and Sn are below the critical magnetic field in Type I conductors (Hc>H) and are shielded due to the Meissner effect.

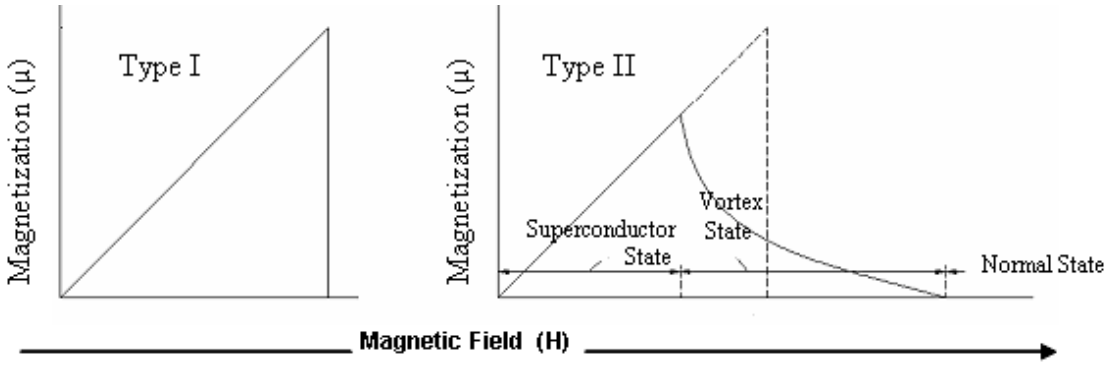

Figure 2.4. Magnetic Shielding Effect in Type I and Type II Superconductors (Source: Encyclopædia Britannica 2008)

Type II superconductors are determined by two critical fields shown as H_{c1} and H_{c2} in Figure 2.4. If the applied field is smaller than the lower critical field (H_{c1}), the field is totally expelled and the material behaves the same as a Type I superconductor (Sumption, et al. 2004). If the external field exceeds the upper critical field the flux penetrates into the total of the sample and the superconducting state disappears. However, the material for the field between H_{c1} and H_{c2} are found in a mixed state known as the vortex state. When in a vortex state, materials can have zero resistance and the flux can penetrate partially. When the applied field exceeds the lower critical field, the vortex states are formed as fibers composed of normal parts. When the strength of the applied field increases, the number of fibers increases and when it reaches the upper critical field the sample passes to a normal state.

When currents are carried through the Type II superconductors which have been applied magnetic fields, the Lorentz force which tries to push the magnetic flux lines outwards and vertically towards the current, forms. If the magnetic flux lines cannot be totally discarded, heat is produced. This causes the material to warm and the transition

temperature of Tc to fall. But adding impurities and stopping the movements of vortices by flux pinning, it may be possible to form zero resistance for this kind of superconductor. Unfortunately, there are many structural flaws in superconductor materials that let transition of magnetic flux up to a certain critical current value. Generally, it is a very important parameter in applying critical current density instead of critical current.

In 1962, the first commercial superconducting wire was produced by researchers in Westinghouse from niobium and titanium alloys. The same year, Brian D. Josephson proved that there is a tunneling current between two superconductors separated with 2 mm insulator obstacle (Josephson 1962). The characteristic is known as the Josephson effect was benefited from in SQUID (superconducting quantum interference devices) used in perceiving weak magnetic fields.

Scientists have conducted researches for years looking for new materials that show superconductivity in higher temperatures. Until recently, the niobium germanium (Nb_3Ge) alloy was known to have the highest critical temperature (23.2 K). At the beginning of 1986, in the IBM Research Laboratories, in Rüschlikon, Switzerland, J. George Bednorz and Karl Alex Müller made a revolutionary discovery in the field of superconductivity. These researches put forward that lanthanum, barium, copper and oxygen compound is a ceramic superconductor at approximately 35 K. (Bednorz and Müller 1986). Right after this, researches in other laboratories showed that superconducting phase is $La_{2-x}Ba_xCuO_4$ where x=0,2. In another research, it was found that by using strontium instead of barium, the critical temperature of 36 K could be reached. The year of 1986 was considered to be the beginning of research on high temperature superconductivity. At the beginning of 1987, research groups from the Universities of Alabama and Houston, observed superconductivity in a phase comprised of yttrium, barium, copper and oxygen close at approximately 92 K (Wu, et al. 1987). This discovery was verified by groups in other parts of the world and the superconducting phase was determined as $YBa_2Cu_3O_7$. The transition temperature of this compound was a turning point for high temperature superconductivity as it is over 77 K, the boiling point of liquid nitrogen which is found easily and used as a cooler. Maeda and his friends synthesized Bi_2SrCuO_x (Bi-2201), $Bi_2Sr_2CaCu_2O_x$ (Bi-2212), and $Bi_2Sr_2Ca_2Cu_3O_x$ (Bi-2223) ceramic compounds comprised of bismuth, strontium, calcium, copper and oxygen (Maeda, et al. 1988).

Another research on high temperature superconductivity was conducted with the synthesis of Tl-Ca-Ba-Cu-O and the critical temperature of 120 K was reached (Sheng and Hermann 1988). In 1993, the superconducting $HgBa_2Ca_2Cu_3O_8$ was synthesized by adding mercury instead of thallium, and the critical temperature was found to be 133 K (Cantoni, et al. 1993). In this compound, with the superconducting phase compositioned $Hg_{0.8}Tl_{0.2}Ba_2Ca_2Cu_3O_{8+x}$ which was obtained by the partial substitution of thallium for mercury, the critical temperature was increased to 138 K (Dai, et al. 1995). Of course, the final aim is that for humans to able to perform superconductivity at room temperature.

In 2001 Prof. J. Akimitsu found that magnesium boride (MgB_2) which is a metallic superconductor, has a high critical temperature of 39 K, for the first time (Nagamatsu, et. al. 2001). Intense researches conducted for the past few years, shows that electric current of over one million ampere per centimeter square could be passed through at 20 K from these materials and that the superconductivity did not corrupt (Takano, et al. 2001). Magnesium diboride has a high critical temperature and current density and in addition has a low cost. This gives advantage to these materials considerably in terms of applicability among other superconductors. Also instead of working at the temperature of 4.2 K, with liquid helium which is very expensive, by using cryopumps that can go down to 10 K with very little power consumption or the digital cryoelectric technology that is set on the superconductive MgB_2 which can work with liquid neon (15 K) or liquid hydrogen that is a lot cheaper, will contribute to its applicability extraordinarily.

2.2. MgB_2, its Structure and Superconductivity

The superconductivity of MgB_2 that has been known since 1950 was discovered by an undergraduate student in Japan in 2001. Although MgB_2 has a lower critical temperature than other high superconductors that are known today, it is one of the closest superconductors to be used in industry, besides having two times higher critical temperature than the materials such as Nb_3Ge, NbTi which are used in technology nowadays.

MgB_2 has a simple hexagonal AlB_2 type structure with the P6/mmm space group, that is common among borides (Yıldırım 2002). Graphite type boron atoms are placed

among crystal structured hexagonal closed packed magnesium atoms. Each magnesium atom takes place in the centers of the hexagons that boron atoms form and donate their electrons to the boron planes. Magnesium diboride shows a strong anisotropy in the B-B lengths, the distance between the boron planes is importantly longer than in plane B-B distance (Cardwell and Ginley 2003).

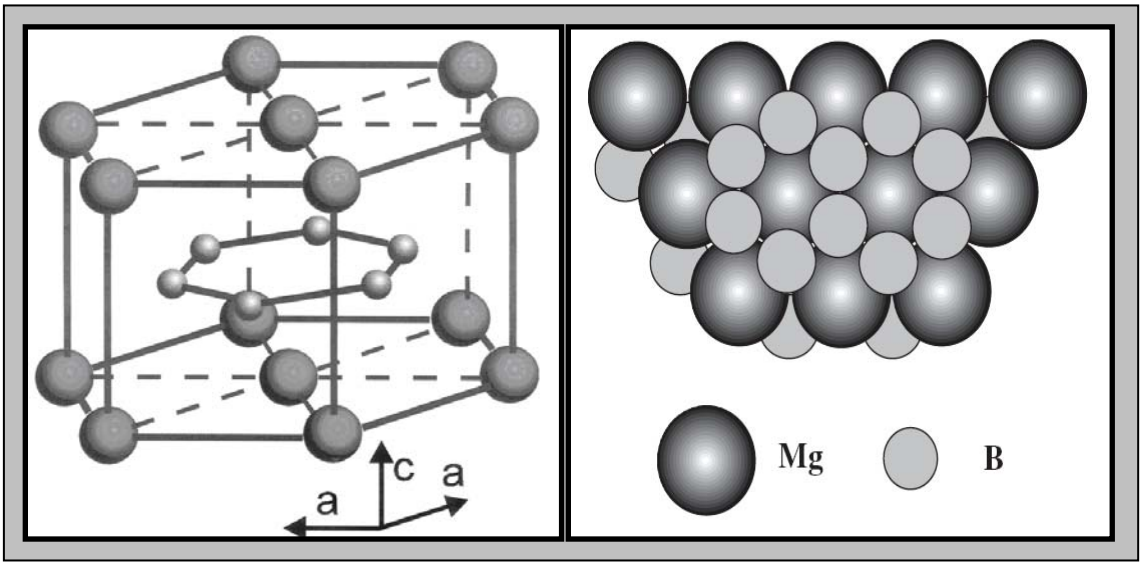

Figure 2.5. The Crystal Structure of MgB_2 and Parallel Layers of Magnesium Metal and Boron Atoms in MgB_2 (Source: Larbalestier, et al. 2001 and Glowacki, et al. 2001)

The hexagonal unit cell has the in plane lattice parameter of a = 0.3086 nm and out of the plane lattice parameter of c = 0.3524 nm, and these values change according to the origin system of magnesium and boron atoms.

The reason why magnesium boride has a high critical temperature (39 K) is that the interaction among certain lattice vibrations with certain electrons is strong. The strong interaction forming here, results from the crystal structure of MgB_2 and connectivity condition of electrons. The electrons responsible for conductivity are considered to be in the boron layers. While there is a very strong connectivity inside the hexagonal planes, there is very weak connectivity among the planes (Kılıç, et al. 2004). The transmission electrons of the interplane bonds are strongly affected by the intraplane lattice vibrations. The interaction mechanism is known to depend on phonon commutation same as the BCS theory. This strong interaction or pairing mechanism maintains the protection of the superconductors at high temperatures.

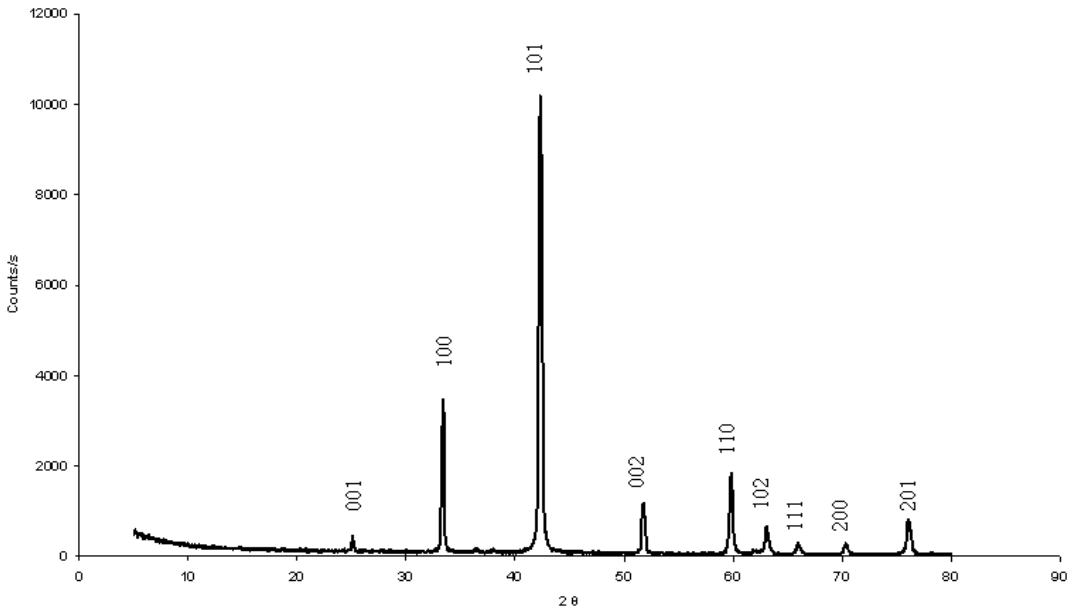

Figure 2.6. XRD Pattern of Commercial MgB_2 Powder from Alfa Aesar

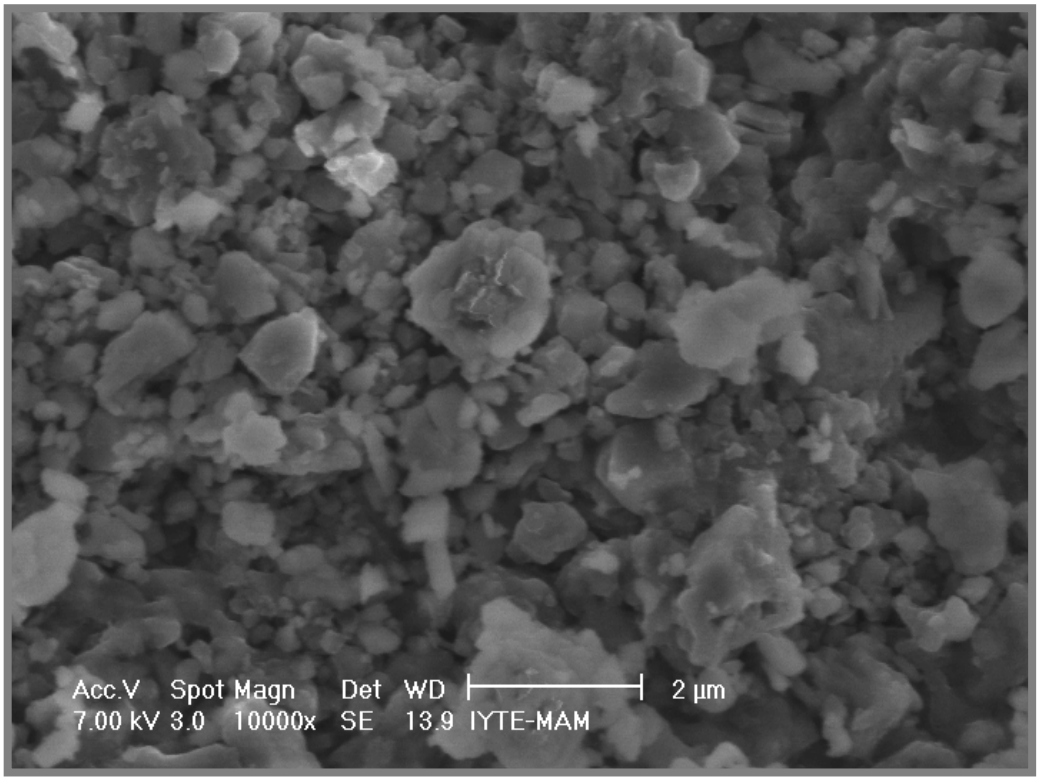

Figure 2.7. SEM Micrograph of Commercial MgB_2 Powder from Alfa Aesar

2.3. Preparation of MgB_2 Samples

2.3.1. Synthesis of MgB_2

MgB_2 is obtained by the solid state reaction between magnesium and boron elements. Mg and B, which are mixed in certain proportions, are annealed for a certain time in argon atmosphere at high temperatures. In this study, the sintering was done at four different temperatures (700-750-800-850°C), and sintering time was taken as 30 minutes.

$$Mg + 2B \xrightarrow[Ar]{700\text{-}750\text{-}800\text{-}850^{\circ}C} MgB_2$$

There are many factors that affect the cost and quality while producing MgB_2. One of these is the quality of the Mg and B elements that are used as precursor materials. Another factor is the proportions of the Mg and B to form MgB_2. Hinks worked on the effect of the different stoichiometric coefficients of Mg and B during the sintering process (Hinks, et al. 2002). In his works, Hinks formulized the excess and inadequate Mg amounts as (Mg_xB_2) $0.5 \geq x \geq 1.3$. A similar research was carried out by Ribeiro and was observed that when the Mg amount is inadequate, the phase of MgB_4 is formed (Ribeiro, et al. 2002). In both researches, the maximum transition temperatures was obtained when x=1 for Mg_xB_2. In this research, the Mg percentage was increased by 0-5-10-15%, compared to stoichiometric ratio.

2.3.2. Preparation of Superconducting MgB_2 Wires

Since MgB_2 is in a powdered form as a precursor material, this material has to be transformed into wire and tape before using in technological applications. To be able to produce wire from MgB_2 which has a very low fragile endurance, some necessary techniques are needed. The most common method to produce wire from fragile powders is the powder in tube method (PIT). Other than the powder in tube method, there are also metal matrix composite method and the continuous tube forming and filling method (Soltanian 2004).

2.3.2.1. Powder In Tube (PIT) Method

Powder In Tube method is one of the most commonly used methods to produce wire and tape out of fragile powdered material. The PIT method has advantages such as low cost, easy formation and the suitability for large scale industrial applications.

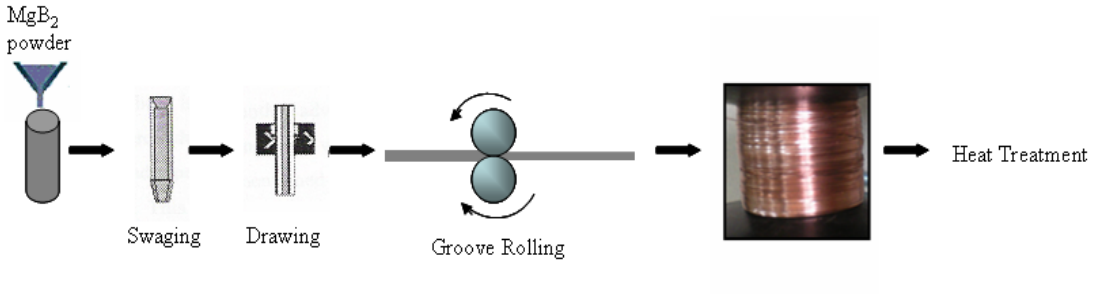

Figure 2.8. Schematic Representation of Powder In Tube Method
(Source: Flükiger, et al. 2003)

More importantly, it is the only method to produce multi-filament wire and tapes. With this method, the fragile superconductive powders are filled in a ductile metal tube. Then, as it is shown in Figure 2.8, it is extended by groove rolling or drawing into small diameters.

Wire and tape was produced with or without using heat treatment with the PIT (Serquis, et al. 2005, Xu, et al. 2005, Kovac, et al. 2006, Salama and Fang 2007, Hishinuma, et al. 2007, Ye, et al. 2007). The protection of the critical temperature and critical current density during the mechanical formation or sintering to increase mechanical characteristics is considered the basis of the PIT method.

2.3.2.2. Metal Matrix Composite (MMC) Method

In Metal Matrix Composite method, mixed materials are generally produced by putting together a low durable matrix and solid, fragile, high durable ceramic parts. An isotropic composition is formed between the superconducting MgB_2 phase and ductile metallic phase (Özkan 2007). The metal improves fracture toughness and ductility and crack arrest, and in addition behaves as a heat and electric conductor when there is localized breakdown in the superconductivity in the MgB_2 phase when the MMC

method is used which is advantageous (Soltanian 2004). The same particle constituent improves the elasticity coefficient and hardness. The MMC method is commonly used in Ag matrix fragile ceramic cuprate and in Cu matrix Ni alloy superconductors. By using the MMC method, Ti powders were mechanically alloyed with 4 wt % MgB_2 at room temperature. At 600°C, a ternary boride phase not exhibiting superconductivity was observed to form. A compacted mixture of MgB_2-11 wt % Al powders was vacuum sintered into a composite demonstrating superconductivity at 38 K in some other studies.

Metal Matrix Composite method is a new method for superconductors. Liquid infiltration and hot pressing techniques are used in order to produce metal matrix composite materials. The MMC method is usually prepared by liquid-metal infiltration where a ceramic perform comprised of packed powders, whiskers or fibers is infiltrated mostly under pressure in order to overcome capillary forces by a metallic melt that is later solidified (Yavaş 2004). Dunand and Giunchi prepared metal matrix composite materials by the liquid infiltration method using Mg metal phase (Dunand 2001, Giunchi, et al. 2002). Dunand carried out infiltration by using both commercial MgB_2-liquid Mg and reactive B powders-liquid Mg.

2.3.2.3. Continuous Tube Forming and Filling (CTFF) Method

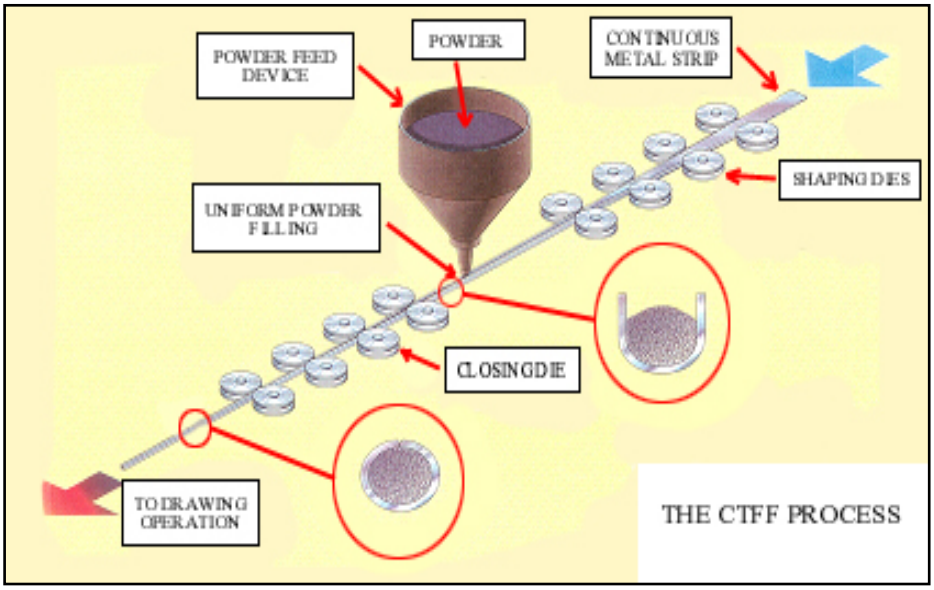

Figure 2.9. Schematic Representation of the CTFF Method
(Source: Hyper Tech Research, Incorporation 2008)

This technique has been used in America for the production of MgB_2 wire and tape by the Hyper-Tech group. In continuous tube forming and filling technique, the continuous metal strip (Fe, Cu) was produced as a sheath material. The metal ribbon first goes through the tube shaping dies and then curves resembling a U. After the powder is filled, the closing dies gradually close off the tube. The diameter of the powder filled metal tube that becomes a cylinder is reduced to 2 mm with a drawing process.

2.3.3. Effect of the Sheath Material

The reaction that may occur between the superconducting phase and the sheath material during the production of superconducting wires is important. So, in the production of MgB_2/metal composite wires with the PIT method, Suo and his friends used Fe (Suo, et al. 2002, Collings, et al. 2003), Glowacki et al. (2001) Ag, Tanaka et al. (2002) Ni, Soltanian et al. (2003) Cu, Xu et al. (2005) and Vinod et al. (2007) stainless steel as sheath materials. Among sheath materials iron is used in the production of superconducting wires as it is economical, provides magnetic shielding

against external magnetic fields and it does not react with MgB_2 (Wang, et al. 2001). Also, even though it is sintered at 900°C, that MgB_2 still exhibits a high critical current density of $1{,}42.10^5$ A/cm^2 (4.2K) makes Fe one of the best sheath material (Feng, et al. 2003). Copper is also used as a sheath material as it is cheap as well as being easily deformed; however it drops the critical current density to certain levels as it interacts with copper superconducting core MgB_2 at the high temperature sintering process (Xiang, et al. 2003). In addition, Nb and Ta sheaths were tried in order to prevent the reaction of boron or magnesium with sheath material (Goldacker, et al. 2001, Feng, et al. 2003, Fu, et al. 2003, Kovac, et al. 2006).

2.3.4. Effect of the Precursor Material

In terms of precursor material, two main different methods as in-situ and ex-situ reactions are used in the production of the superconducting MgB_2.

2.3.4.1. In-Situ Reaction Technique

In the *in-situ* reaction technique, after filling the unreacted Mg and B powders into a metalic tube, MgB_2 is obtained as a result of heat treatment conducted at high temperature (Wang, et al. 2001, Machi, et al. 2003, Soltanian, et al. 2003, Collings, et al. 2003, Sumption, et al. 2004, Shimura, et al. 2004, Feng, et al. 2004, Bhatia, et al. 2004, Xu, et al. 2005, Higashikawa, et al. 2005, Sumption, et al. 2005, Kovac, et al. 2006, Jiang, et al. 2006, Salama, et al. 2007, Tomsic, et al. 2007, Musenich, et al. 2007, Yamamoto, et al. 2007, Hishinuma, et al. 2007, Ye, et al. 2007, Vinod, et al. 2007, Zhao, et al. 2008, Mudgel, et al. 2008). In this study, *in-situ* reaction technique was used, too.

2.3.4.2. Ex-Situ Reaction Technique

In the *ex-situ* reaction technique, the MgB_2 powder is filled into an appropriate metal tube, then it is formed into a wire by drawing or groove rolling (Tanaka, et al. 2002, Ahoranta, et al. 2004, Musenich, et al. 2004, Cambel, et al. 2005, Serquis, et al.

2005, Sumption, et al. 2005, Kitaguchi, et al. 2006, Stenvall, et al. 2007, Ye, et al. 2007).

The ex-situ reaction technique is appropriate for small and homogeneous micro structures. This technique is very sensitive to doping and sometimes for some doping, even a 1% change can corrupt the superconductivity. The in-situ technique is a more advantageous technique because it lets in doping and sheath types.

2.3.5. Effect of the Annealing Temperature

The sintering process decreases the porosity and increases the connectivity between particles, therefore provides a more homogeneous structure. As a result, while the Tc critical transition temperature increases, the critical current density increases too. The effect of the annealing temperature on the critical transition temperature is shown in Figure 2.10. According to this, the Tc critical transition temperature gradually increases while the annealing temperature increases. Also, as shown in the SEM image in Figure 2.11, as the annealing temperature increases the pores gradually close.

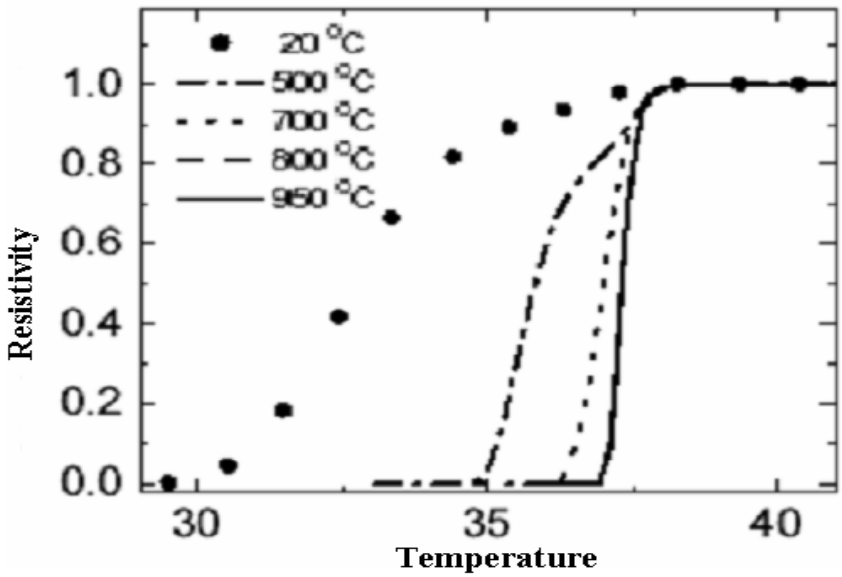

Figure 2.10. Effect of Annealing Temperature on Superconducting Resistivity (Source: Jung, et al. 2001)

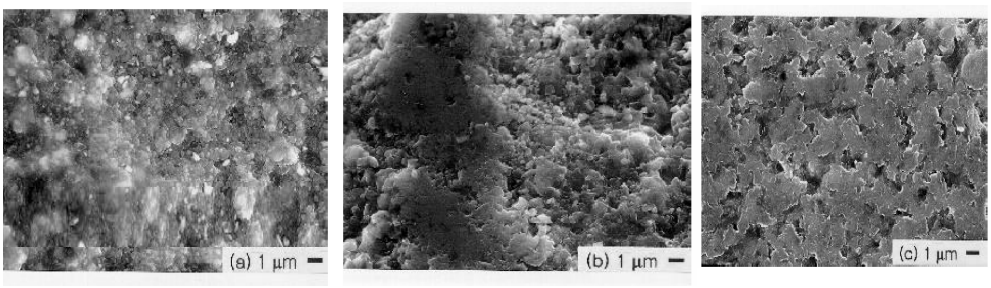

Figure 2.11. SEM Micrographs of MgB_2 Samples Heated under 3 GPa. Annealing Temperatures a) 20 ^oC, b) 500 ^oC, and c) 950 ^oC (Source: Jung, et al. 2001)

The annealing temperature changes depending on the way the samples are prepared. In a study, it was found that the wires that are prepared with the ex-situ technique need heat treatment at approximately 950°C, wires prepared with the in-situ technique complete the reaction at lower temperatures (600-750°C) (Dou, et al. 2003, Fu, et al. 2003).

2.3.6. Effect of Chemical Doping

The magnitude of the powder particles used is very important in terms of the connectivity among the particles. Weak connectivity among particles prevents the movements of the magnetic flux and heats the material. This is a factor which affects the superconductivity in a negative way. Metallic doping are usually very effective in increasing the conductivity and the connectivity among particles (Zhao, et al. 2001, Ma, et al. 2003, Dou, et al. 2003, Sumption, et al. 2005, Pachla, et al. 2006). Figure 2.12 shows the effects of the doping materials used in literature on the Tc critical transition temperature. According to this, while Zn, Si and Li are not very effective, Mn, Al and C are very much effective.

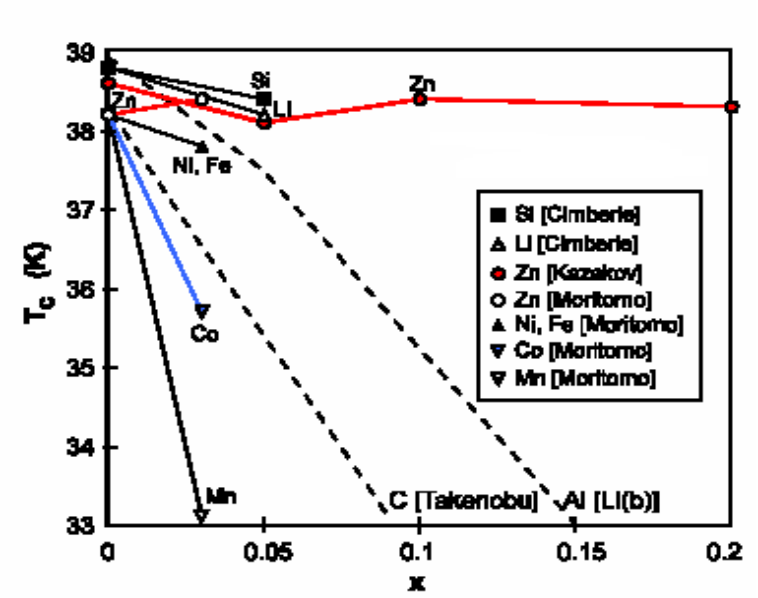

Figure 2.12. Effect of Chemical Doping on the Critical Transition Temperature (Source: Okur 2005)

Ti or Al that are used with MgB_2 fill in the gaps between particles and connect the particles to each other (Fu, et al. 2003). Ti is used as a doping material because it is similar to magnesium diboride with its hexagonal crystal structure and has a smaller volume and also it is a good conductor which has a high fusion temperature, due to these the critical current density has increased largely (Gencer, et al. 2005, Yavaş, et al. 2005, Okur, et al. 2005).

Mg that is used as a doping material is soft and has a low fusion temperature therefore it can easily penetrate into the MgB_2 and form connectivity among particles (Eğilmez, et al. 2004, Okur, et al. 2005). Also, the extra Mg doping, prevents the corruption of superconductivity by protecting the chemical composition of the magnesium diboride that is formed by the Mg diffusion in the superconducting core during the formation of the $MgCu_2$ layer forming in the inner walls of the copper sheathed wires during the high temperature sintering process (Eğilmez, et al. 2004, Soltanian, et al. 2002).

Another research conducted in order to increase the critical current density is Zr doping. In the samples prepared with different compositions ($Mg_{1-x}Zr_xB_2$), the best critical current density (Jc) values belong to $Mg_{0.9}Zr_{0.1}B_2$ and 2.1×10^6 A/cm^2 (at 0.56 T and 5 K), and 1.83×10^6 A/cm^2 (at 0 T and 20 K) (Feng, et al. 2001).

Wang and his colleagues added 5-10-15 wt % of Y_2O_3 nano particles to the MgB_2 matrix. The result of the experimental studies showed that 10 wt % nano- Y_2O_3

doped samples reached the critical current density of 2.0×10^5 A/cm^2 at 2 T and 4.2 K (Wang, et al. 2002).

In studies conducted with Li, Al and Si doping, while the critical current density increased with Si doping, there was no observation of important decreasing in the critical temperature (Cimberle, et al. 2002).

Canfield and his group showed that superconducting transition decreased to 4 K with 5 wt % carbon doping however the superconductivity did not corrupt until the 36 T high magnetic field (Ribeiro, et al. 2003). This result is very important for superconducting coils that are used to form high magnetic fields. NbSn type alloys could only resist up to 30 T.

Shimura reached the critical current density of Jc= 230 kA/cm^2 corresponding to 208 A at 4.2 K high currency from the TiH_2 doped, copper sheathed MgB_2 wires (Shimura, et al. 2004).

In recent studies on increasing the electromagnetic characteristics of the MgB_2 superconducting tapes, 10 wt % SiC doped samples reached 37 Tesla at 5 K and the critical current density of $5x10^5$ A/cm^2 at 20 K, which is 30 times more than what is reached with MgB_2 that is free from doping (Sumption, et al. 2005).

Serquis, heat treated the wires and coils he doped at 5 wt % Mg and 5 wt % Mg + 5 mol % SiC to two different heat treatments. According to this, hot isostatic pressed MgB_2 wires have a higher critical current density (10^4 A/cm^2 at 8 T) than the wires sintered in high magnetic field and high temperature (Serquis, et al. 2005).

In the studies Kovac and his colleagues conducted, 10 wt % SiC and 10 wt % W doped MgB_2 wires prepared with ex-situ and in-situ techniques were compared in terms of critical current densities, diameters of filaments, number of turns, mechanical characteristics and thermal stability. While the critical current density of the 10 wt % W doped ex-situ wire prepared with a Fe sheath decreases (0-10 T) 10^5 times with the increasing external magnetic field. The critical current density of 10 wt % SiC doped in-situ wire prepared with a Nb/AgMg sheath decreases less than 10^3 times. SiC particles are decomposed during the sintering, and the substitution of boron by carbon increases the upper critical field (Hc_2), therefore the critical current density is improved in high magnetic fields (Sumption, et al. 2005, Pachla, et al. 2006). Mg_2Si and Mg_2SiO_4 phases formed from the interaction of Mg with silicone protect the particle structure of MgB_2 (Pachla, et al. 2006). The presence of tungsten particles affects both thermal conductivity and resistivity of the MgB_2 core, and increases the critical current density

due to the improved internal stability (Kov´aˇc, et al. 2004). Also, in samples prepared with in-situ technique, cracks seen during the heating process were observed to be less than in ex-situ technique.

In another study, Nb/CuNi sheathed, free from doping and Mg-SiC doped monofilament wires and Nb/Cu/CuNi sheathed and Mg doped 18-filament MgB_2 wires were examined in terms of their critical characteristics. Critical currents at 25 K and 0 T were found as 200 A, 238 A, 328 A respectively (Ye, et al. 2007).

Hishinuma added Mg_2Cu at 1 wt % and 3 wt % into the boron and magnesium mixture and filled into the Fe and Ta tubes. The diameters of these tubes were reduced to 1.04 mm and were sintered for a very long time (100-700 hours) in Ar atmosphere at 400-500°C. As a result, the maximum critical current density was found to be about $1.8x10^5$ A/cm^2 by the longer-time heat treatment at 450 °C for 200-300 hour (Hishinuma, et al. 2007).

In this study, the effects of the Mg doping were analyzed. Because Mg is a very soft material, it plays an important role in putting powdered ductile MgB_2 particles back together, increasing superconductivity and the elasticity of the material.

2.3.7. Critical Field

That the critical temperature of MgB_2 is higher, it has more advantages in terms of today's approachable technology that is designed according to the boiling point of liquid helium. The primary advantage is that, it gives way to using cheaper and economical cooling systems. When looked from the engineering point of view, besides high temperatures, it is important that superconducting devices work in high magnetic fields. In superconducting form, the critical current density of MgB_2 forms different magnetic fields with samples of wires, tapes, bulks and thin films. At temperature measurements of 4.2 K and 20 K, critical current densities formed under different magnetic fields such as 2T, 4T, 6T and 8T are shown in Table 2.1.

Table 2.1. Effect of Magnetic Field on the Critical Current Density
(Source: Yavaş 2005)

4.2 K					
	Sheath Material/Doping	J_c (A/cm^2) 8 T	J_c (A/cm^2) 6 T	J_c (A/cm^2) 2 T	References
Wire	Ta, Cu			2.10^4	Canfield, et al. 2001
	Cu		10^4	6.10^4	Eisterer, et al. 2002
	SS		2.10^4	10^5	Serquis, et al. 2003
	Fe		2.10^4	10^5	Dou, et al. 2003
Film	Al_2O_3	5.10^4	10^5	2.10^6	Bu, et al. 2002
	$SrTiO_3$	$1.6.10^5$	$2.7.10^5$	8.10^5	Eom, et al. 2001
	YSZ	10^5	2.10^5	2.10^5	Komori, et al. 2002
Bulk	-	10^2	6.10^2	10^4	Flukiger, et al. 2003
	-		10^2	5.10^4	Wang, et al. 2002
20 K					
	Sheath Material/Doping	J_c (A/cm^2) 4 T	J_c (A/cm^2) 2 T	J_c (A/cm^2) 0 T	References
Wire	Fe	2.10^3	5.10^4	5.10^5	Suo, et al. 2002
	Ta			2.10^5	Canfield, et al. 2001
	SS		10^5		Giunchi, et al. 2002
Film	Al_2O_3		4.10^4	2.10^6	Pradhan, et al. 2001
	$SrTiO_3$		$1.7.10^5$	2.10^6	Eom, et al. 2001
	Al_2O_3			7.10^6	Moon, et al. 2001
Bulk	-	5.10^3	3.10^4	7.10^5	Kim, et al. 2002
	-	10^3	7.10^3	8.10^4	Zhao, et al. 2002

The critical current densities of NbTi and Nb_3Sn that are used in technology at zero field and 8 Tesla are 10^7 A/cm^2, 8.10^4 A/cm^2 ve 10^7 A/cm^2, 10^5 A/cm^2, respectively at 4.2 K. When we look at the critical current densities of wire and bulk MgB_2 samples from Table 2.1, we see that the values of the critical current density at 20 K is lower it than at 4.2 K.

Many groups work on the chemistry and stoichiometry of MgB_2. When different elements such as Li, Na, Ca, Ag, Cu, Al, Zn, Zr, Ti, Mn, Fe, Co and C are added or used as sheath materials, the connectivity of the critical current density to the magnetic field is analyzed. While all the elements named above cause the transition temperature to decrease when they are added, the addition of Ti, Zr_2O and SiC when magnetic field is not applied or especially when it is applied, an increase in the critical current density is observed.

Table 2.2. Literature Review

Material / Sheath Material	Length (m) / Outer Diameter (mm)	Temperature (K) / Magnetic Field (T)	Current (A) / Current Density (A/cm^2)	References
MgB_2/Ni tape	-	4.2 K / 0 T	- / $3x10^5$ A/cm^2	Grasso, et al 2001
In-situ MgB_2/Fe coil & wire	-	15 K / 0 T	- / $4.5x10^5$ A/cm^2	Wang, et al 2001
		15 K / 2 T	- / $>10^5$ A/cm^2	
Ex-situ MgB_2/Ni coil	10 m (80 turns) / 1 mm	4.2 K / 0 T	105 A / $5x10^4$ A/cm^2	Tanaka, et al 2002
In-situ MgB_2/Cu coil	3.5 m (50 turns) / 0.5 mm	4.2 K / 0.37 T	200 A / $4.4x10^5$ A/cm^2	Machi, et al 2003
In-situ MgB_2/Cu	1 m (5 turns) / 1 mm	4.2 K / 0 T	72 A / $1.33x10^5$ A/cm^2	Soltanian, et al 2003
	1 m (100 turns) /1 mm		100 A / -	
In-situ MgB_2/Cu coil	42 m (80 turns) /1 mm	4.2 K / 0 T	120 A / $6.12x10^4$ A/cm^2	Sumption, et al 2004
In-situ MgB_2/Fe coil	4 m / 1 mm	4.2 K / 1 T	185 A / -	Feng, et al 2004
In-situ MgB_2/Cu coil	18 m / 1mm	20 K	360 A / $1.8x10^5$ A/cm^2	
In-situ MgB_2/Cu coil	20 m (170 turns) / 1 mm	4.2 K / 0 T	278 A / -	Hascicek, et al 2004
Ex-situ MgB_2/SS	6 layered helical	25 K / 1 T	220 A / $2.8x10^4$ A/cm^2	Serquis, et al 2004
	25 m / 1 mm	4.2 K / 0 T	350 A / $4.5x10^4$ A/cm^2	
In-situ MgB_2/Cu	1 m helical / 1 mm	4.2 K / 0 T	- / $1.3x10^5$ A/cm^2	Bhatia, et al 2004
In-situ MgB_2/Fe	18 m square wire	20 K / 0 T	360 A / -	Salama, et al 2007
		20 K / 1 T	159 A / -	
		25 K / 0 T	260 A / -	
		25 K / 1 T	110 A / -	
		30 K / 0 T	157 A / -	
		30 K / 1 T	51 A / -	

2.3.8. Strong Grain Connectivity

MgB_2 is good in terms of the connectivity among its particles compared to other high temperature superconductors (absence of weak links), therefore grain boundaries are highly transparent to current flow (Larbalestier, et al. 2001, Kambara, et al. 2001). This is an advantage of MgB_2 compared to the HTS superconductors so far as practical applications are concerned, since high values of critical current density have been observed in MgB_2 thin film, bulk, tapes and wires with no weak links.

CHAPTER 3

MATERIALS AND METHODS

3.1. Sample Preparation

3.1.1. Synthesis of MgB_2

The discovery of 40 K superconductor MgB_2, has stimulated interests due to its simple binary chemical composition, and its high critical temperature compared to other metallic superconductors. Hence, the principal goal of this study was to synthesize MgB_2 that would lead to new possibilities of practical applications.

Samples of MgB_2 were prepared through the solid state reaction using powder in tube method following the in-situ process. Specifications of the samples of MgB_2 wires are listed in Table 3.1. Boron powders with purity of 90% (Boronsan Boron), first produced in Turkey by the high temperature electolysis process of sodium borates (Yıldıran, 2006) and commercial amorphous boron with purity of 95-97% (AB Boron) were used as boron sources. For sample A, stoichiometrically weighed magnesium (99.8% purity, -325 mesh, Alfa Aesar) and boron powders (95-97% purity, AB) were well mixed in a Retsch S1000 series ball mill for 3 h, and doped with 5% Mg powder. Similarly, for sample B powders of magnesium (99.8%, Alfa Aesar) and boron (90%, Boronsan) with the stoichiometric ratio of MgB_2 were uniformly mixed through the grinding for 3 h, and 5-10-15 wt% of extra Mg were added to the in-situ powders. During all grinding processes, inert medium was provided by Ar gas in order to avoid air oxygen. For this purpose, the grinding system was modified. A 320 mL stainless steel cup with lid was built as a reactor. The lid has two valves for gas inlet and outlet, and the cap is screwed to the main body with six screws. Grinding process was performed with a metal disc with a diameter of 75 mm. The mixed powders were filled into Cu tubes, and also light coloured and dark coloured Fe tubes in the presence of Ar gas, and the diameter of these tubes was reduced down to 1 mm with cold-drawing (groove rolling) process. There was no annealing during the rolling process.

Table 3.1. Specifications of the Samples of MgB_2 Wires

Items	Sample A	Sample B
Type	MgB_2 monofilament	MgB_2 monofilament
Composition	Mg (99.8% Alfa Aesar) + 2B (95-97% AB)	Mg (99.8% Alfa Aesar) + 2B (90% Boronsan)
Chemical Doping	5 % Mg doped	5-10-15 % Mg doped
Sheath Material	copper, light coloured iron, dark coloured iron	copper, light coloured iron, dark coloured iron
Process	in situ	in situ
Annealing	700-750-800-850°C, 30 min.	700-750-800-850°C, 30 min.
Shape	square	square
Cross-sectional	1 mm in diameter	1 mm in diameter
Length	50 mm	50 mm

3.1.2. Fabrication of MgB_2 Wire

3.1.2.1. In situ Synthesis of MgB_2 Wire Using the Powder in Tube Method

In this study, Cu and two types of Fe sheathed MgB_2 wires were fabricated by commonly used powder in tube method due to low material costs and simple deformation processes. Powder in tube method is principally performed in three steps. First step is to prepare the starting mixture and to fill the mixture into the ductile metal tube. Accordingly prepared Mg and B mixture were filled in Cu, light coloured and dark coloured Fe tubes (10 cm in length), with an outside diameter of 8 mm and a wall thickness of 1.5 mm (Figure 3.1.a.).

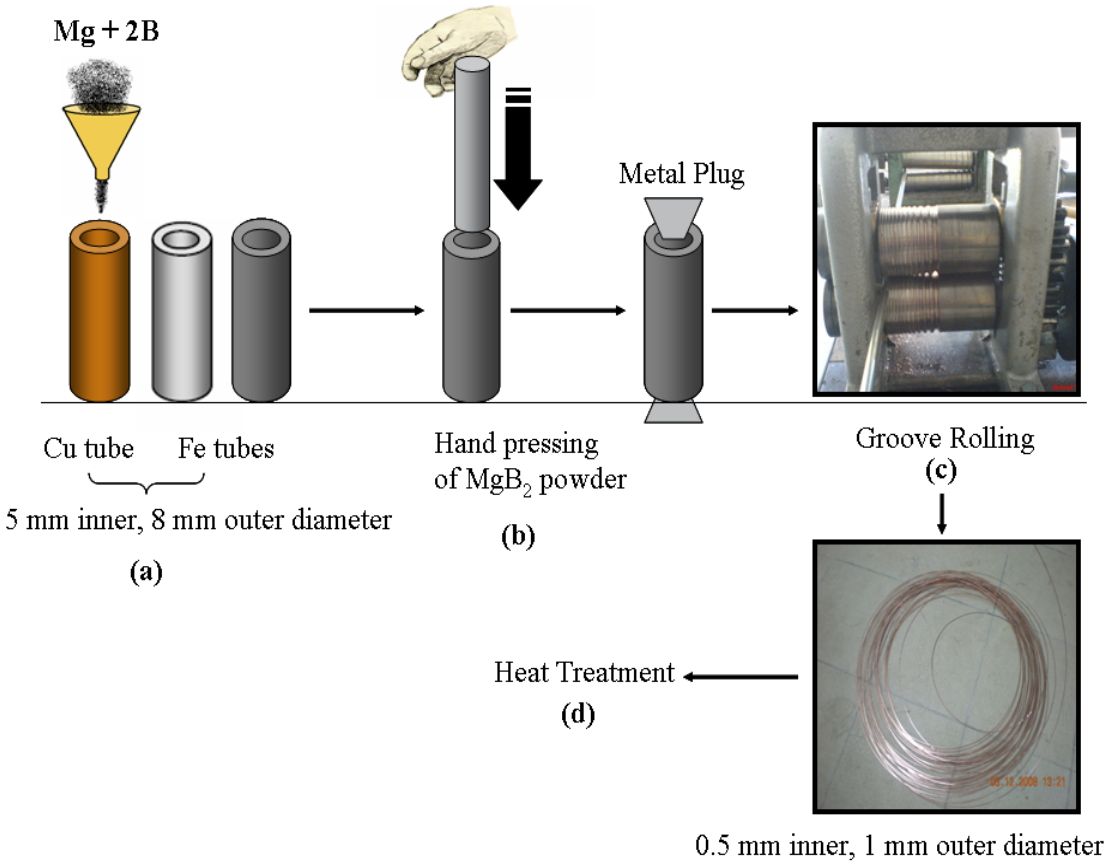

Figure 3.1. Fabrication of the Monofilament MgB_2 Wires

Secondly, hand pressing is required to densify the MgB_2 powder inside the tubes (Figure 3.1.b.). All filling and hand pressing processes were performed in Ar atmosphere in order to avoid air oxygen. Then, the ends of the tubes were closed with a metal plug, and were swaged with a groove roller. The following step is to reduce the diameters of the tubes which lead to increase in the wire length by using groove rolling mill with 12 different groove sizes from 8 mm to 1 mm (Figure 3.1.c.). During this step, small pieces of wires with an outside diameter of 2 mm were cut off in order to obtain enough samples for XRD analysis. Then, groove rolling process was gradually continued to get a wire with a square cross section of about 1 mm. Finally, pieces of wires of 5 cm in length were cut off and heat treated (Figure 3.1.d.) in a tube furnace and in an Ar gas flow under ambient pressure at different temperatures to see the effect of heating temperature.

3.1.2.2. In situ Synthesis of Multifilament MgB_2 Wire

Powder in tube method is the way of producing multifilament wires. To produce multifilament wire, numbers of monofilament wires of 2 mm in diameter are inserted into new metal tube. Then, this tube is mechanically deformed to a smaller size and annealed in a similar process with the monofilament wire.

In this study, to prepare four filament MgB_2 wire with a length of about 200 m, four pieces of monofilament copper clad wires, each about 4 m in length and 2 mm in diameter, were inserted into a copper tube that had 5 mm inner and 8 mm outer diameter. Groove rolling process was repeated to reduce the diameter of four filament wire about 1 mm outside diameter.

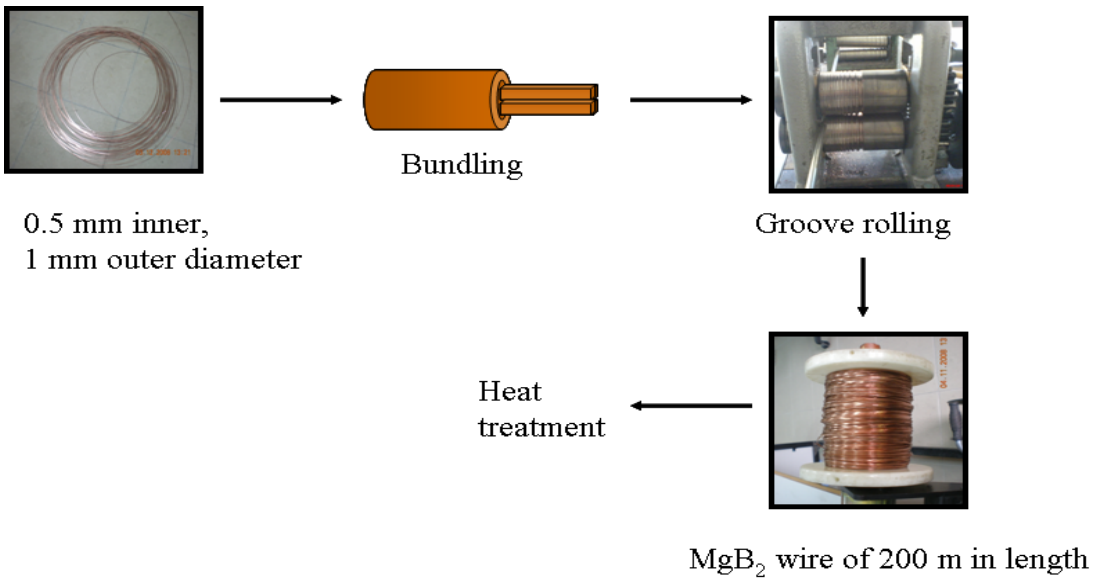

Figure 3.2. Fabrication of the Multifilament MgB_2 Wires

3.1.3. Annealing Process

The filled and drawn wires of 50 mm in length were annealed for 30 minutes at different temperatures ranging between 700°C to 850°C. Heat treatment was performed under Ar gas flow at ambient pressure using a horizontal electric hinged furnace (Thermo Electron Corporation Lindberg/Blue M).

Figure 3.3. Annealing System

The hinged furnace has the maximum temperature limit of 1200°C. The annealing system used in this experiment is composed of a power supply, which has the voltage ranges between 208/240 volts and 30 amps input.

Regarding the working principle of this system, firstly it is important to decide the set point of the temperature. After deciding the annealing process temperature, the system was set to the desired temperature for heating up. After the temperature was stabilized, the system was left for 5 to 10 minutes. Then, the temperature was set to the desired temperature for suitable time and then it was left to cool down the room temperature. The most essential step here was to utilize a rapid cooling process. A temperature profile for the annealing of MgB_2 wires is shown in the Figure 3.4.

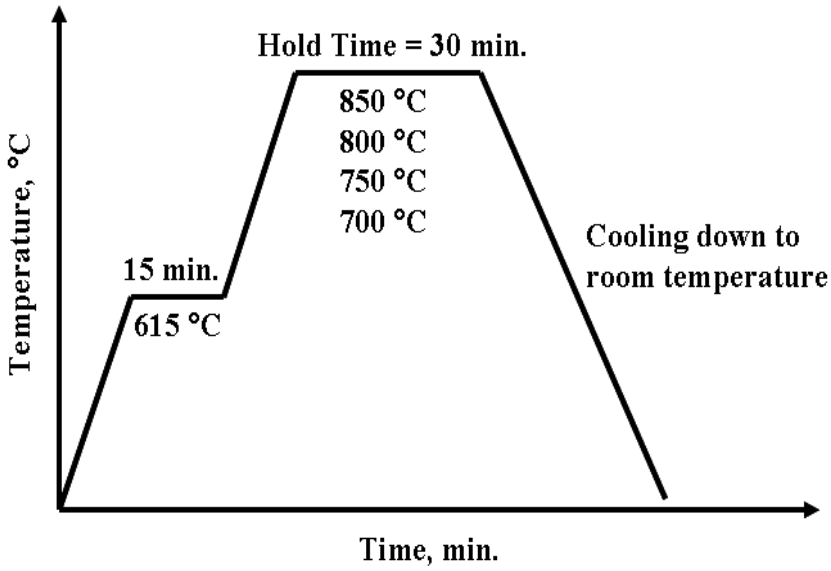

Figure 3.4. A Temperature Profile for the Annealing of MgB_2 Wires

3.2. Characterization Techniques

3.2.1. X-Ray Diffraction (XRD) Technique

The X-ray diffraction technique is the quickest and the most favorable method that brings out detailed information about chemical composition and crystallographic structure of MgB_2 superconductor. This technique is generally used, in order to examine the microstructure, phase formation, and analysis of the texture, as well as calculation of the lattice parameters. The X-ray examinations were carried out using a Philips X'Pert Pro diffractometer. In all X-ray investigations, monochromatized Cu Kα radiation, having wavelength λ=0.154 nm, with the 2θ range of 5° to 100° was used. For phase analysis of MgB_2 wires, samples were obtained from the core of the wire after the metal sheaths were mechanically removed. For the X-ray studies, powders were grinded using a mortar and pestle and the samples were prepared by compressing in the cassette sample holder without any adhesive substance.

3.2.2. Scanning Electron Microscopy (SEM) and Optical Microscopy (OM)

Scanning electron microscope (SEM) is designed to provide high resolution and high magnification micrograph of a sample. SEM uses a high energy beam of electrons which can be scanned in a raster on the sample surface. The electrons interact with the atoms that constitute the sample, generating signals that include information about the sample's surface morphology and composition. SEM characterization was performed using a Philips XL-30S FEG type instrument at IZTECH-Center for Materials Research. Micrographs of the sample surfaces were recorded at different magnifications. Main components, and elemental distribution of samples were analyzed using Energy Dispersive X-Ray (EDX) detector. Prior to analysis, the powder samples were sprinkled onto Al or C tapes which are adhesive and supported on metallic disks. In addition, wire samples were sticked onto the metallic disks with the aid of metal repair tape in order to get the images of wires and measure their diameters.

An investigation of sample morphology can also be made by using a Leica DM2500 M type Optical Microscope (OM) which uses visible light and a system of lenses to magnify images of small samples. OM and SEM differ in terms of depth range and resolution. Optical microscope has smaller depth range and lower resolution with respect to scanning electron microscope.

3.2.3. Resistivity-Temperature (R-T) and Voltage-Current (V-I) Measurements

When superconducting materials pass from normal state to superconductor state at critical temperature, they behave like a diamagnet and their electrical resistivity becomes zero. The resistivity-temperature and voltage-current characteristics of the MgB_2 wires were measured by the standard four point probe (4PP) method, with the sample completely immersed into liquid helium. Short pieces, about 40 mm in length of each fabricated conductor have been measured. 4PP technique which has proven to be a convenient tool for this purpose involves bringing four probes at known distance and geometry into contact with the material of unknown resistance (Institute of Experimental Physics 2008). The wires were connected from four points which are collinear. Current and voltage leads were directly soldered to the surface of the sheath material with a distance of approximately 20 mm between them. Current was applied from the outer probes and voltage drop was measured from the inner probes as shown in Figure 3.4.

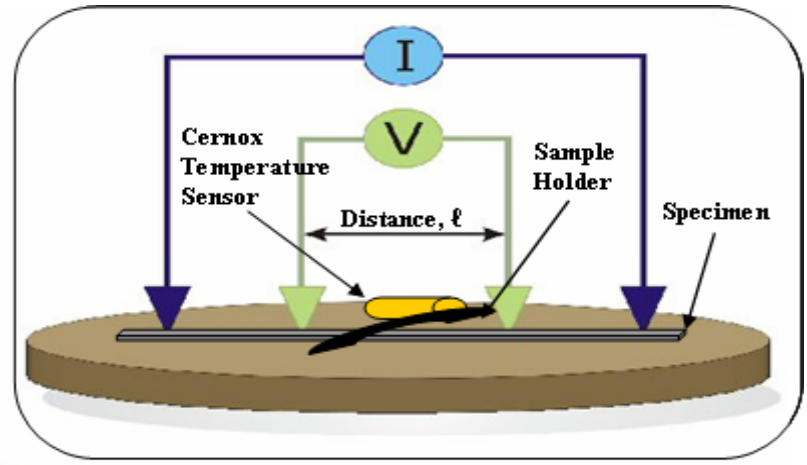

Figure 3.5. Four Point Probe Method
(Source: Institute of Experimental Physics 2008)

When a high impedance voltmeter is connected to the terminals used for measuring the voltage, only a little current is allowed to pass through. These terminals are distinct from those used for passing the main part of the current through the specimen, where voltage drops in both leads and contacts are significant. Temperature of samples was measured by temperature sensor near the specimen and well connected on the surface of probe.

The voltage-current characteristics show the relationship between the DC current through an electronic device and DC voltage across its terminals. The *V-I* characteristics of the MgB_2 wires were measured at 4.2 K in self field for the different sheath materials employed. High current between 0 and 400 A was applied on the superconducting wire and coming voltage values observed by Keithley 2000 multimeter at the temperature of liquid helium.

All data were controlled by IEEE 488.2 interface cards for the connection to the computer. The data acquisition software was written in Objectbench. The corrections for thermal emf's by reversing the current at each reading was done by the software.

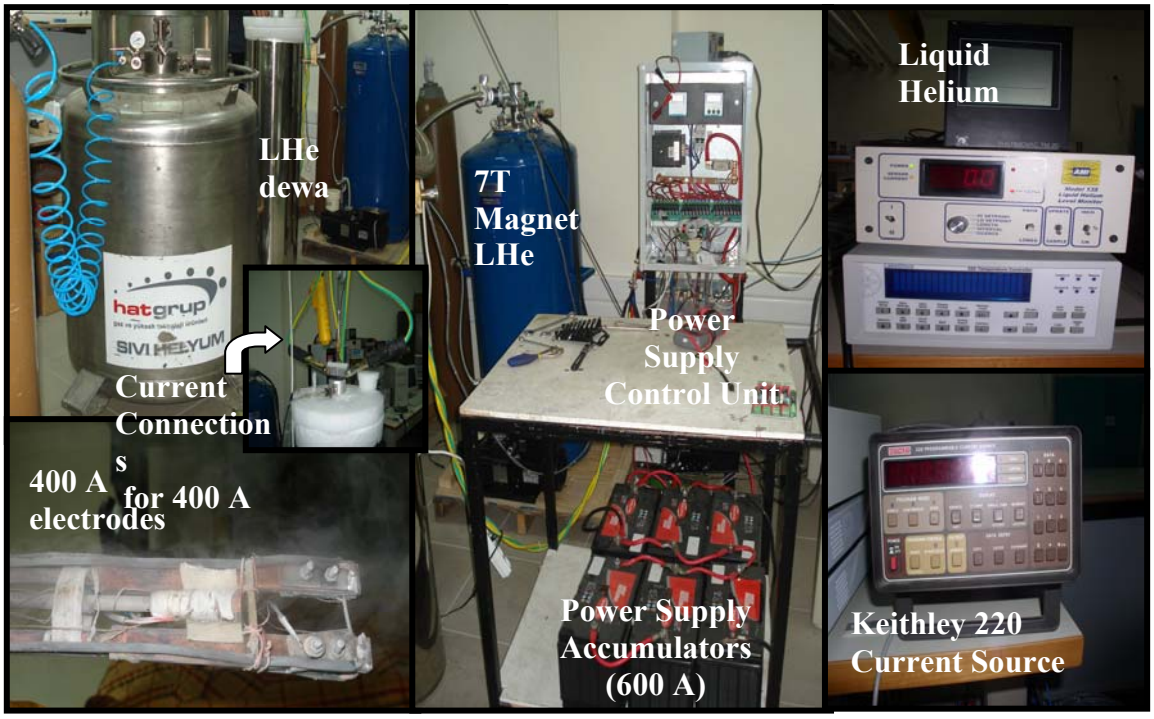

Figure 3.5. 7T Superconducting Magnet Liquid Helium Cryostat System (CryoIndustry)

CHAPTER 4

RESULTS AND DISCUSSION

In this study, the effects of precursor boron powder on the reaction between Mg and B, and their influence on the superconducting properties of MgB_2 were investigated. In the first part of the study, MgB_2 synthesis using commercial magnesium powder and AB boron powder (95-97% purity), and microstructural and electrical characterization of the product was achieved. Effects of sheath material and annealing temperature were also investigated.

In the second part, MgB_2 synthesis using commercial magnesium and Boronsan boron (90% purity) -first produced in Turkey by the high temperature electolysis of sodium borates- was tried. Effect of the annealing temperature and additional chemical doping were examined. Temperature dependence of resistance of MgB_2 wires produced by PIT method and their electrical and microstructural characterization were done through XRD, OM, R-T and V-I measurements.

In the third part, in situ MgB_2 wire 200 m long was fabricated.

4.1. Results of Magnesium Diboride Synthesis

4.1.1. AB Boron used as a Precursor Boron Powder

The effect of the sheath material and annealing temperature was studied in relation to the enhancement of superconducting performance of widely known MgB_2 superconductor. In addition, magnesium addition provides intergranular connectivity because of its softness and low melting point, (Eğilmez, et al 2004, Okur, et al 2005) therefore magnesium was used as a doping material. For this purpose, stoichiometrically weighed magnesium (99.8% purity, -325 mesh, Alfa Aesar) and boron powders (95-97% purity, AB) were well mixed, and doped with extra 5 wt % Mg powder. This powder mixture was then milled by a ball mill for 3 hours for well mixing purposes.

4.1.1.1. Effect of the Sheath Material

The nature and toughness of the sheath material has a strong influence on the formation of MgB_2 superconducting phase, consequently to the critical current and transition temperature. Degradation of superconducting properties in MgB_2 by addition of Cu into the ex-situ MgB_2 core (Aksan, et al. 2006) and using it as sheath material for in-situ MgB_2 wires has been reported in the literature and short sintering time was suggested (Soltanian, et al. 2002). However, B. A. Glowacki et al (2002) have reported relatively higher J_c values for Cu-clad MgB_2 wire that was heat-treated at 700^{o}C for 1 h. In this study, the possibility of using commercial soft copper tubes with 5 mm inner and 8 mm outer diameter as a sheath material for MgB_2 wires fabricated by in situ powder in tube method and comparison of their performance with those of the wires stacked in iron sheaths was investigated.

The mixture of Mg and B powder was filled in Cu, and also dark coloured Fe and light coloured Fe tubes in order to investigate the suitable sheath material. XRD patterns of the two different coloured Fe tubes were similar. Figure 4.1. shows XRD patterns for the two types of iron sheath material.

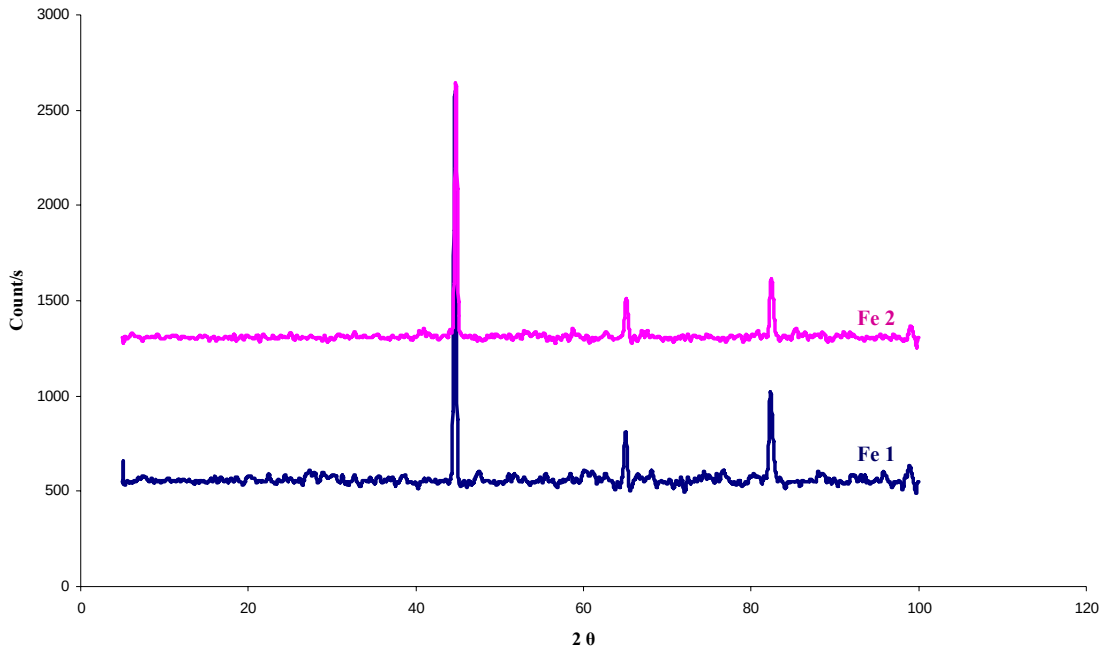

Figure 4.1. XRD Patterns of the Two Types of Iron Sheaths, Fe 1: Light Coloured Iron and Fe 2: Dark Coloured Iron

XRD patterns recorded from the core of the Fe-clad MgB_2 wires after the iron sheath was removed are shown in Figure 4.2. It is clear that, samples consist of MgB_2 as

the main phase, with small amount of MgO. Mg powders or Mg-B mixture used as starting materials were free from oxygen as seen in their XRD patterns. The reason for the formation of small amount of MgO might be due to the entrapped air while filling the tubes. Additonally, MgO might be formed during the heat treatment (Dancer, et al. 2006). The strongest peaks in MgB_2 (2θ = 42.412°) and MgO (2θ = 42.824°) spectra were not used as they overlap severely, such that the MgO peak can not be seperated from the MgB_2 peak. However, MgO peak at 2θ value of 62.167 can be compared with MgB_2 peak at 2θ value of 63.173. Fe1 sheathed sample has higher intensity for MgB_2 peak than for MgO peak. From these results, it can be concluded that light iron sheath is the most suitable sheath material for the processes.

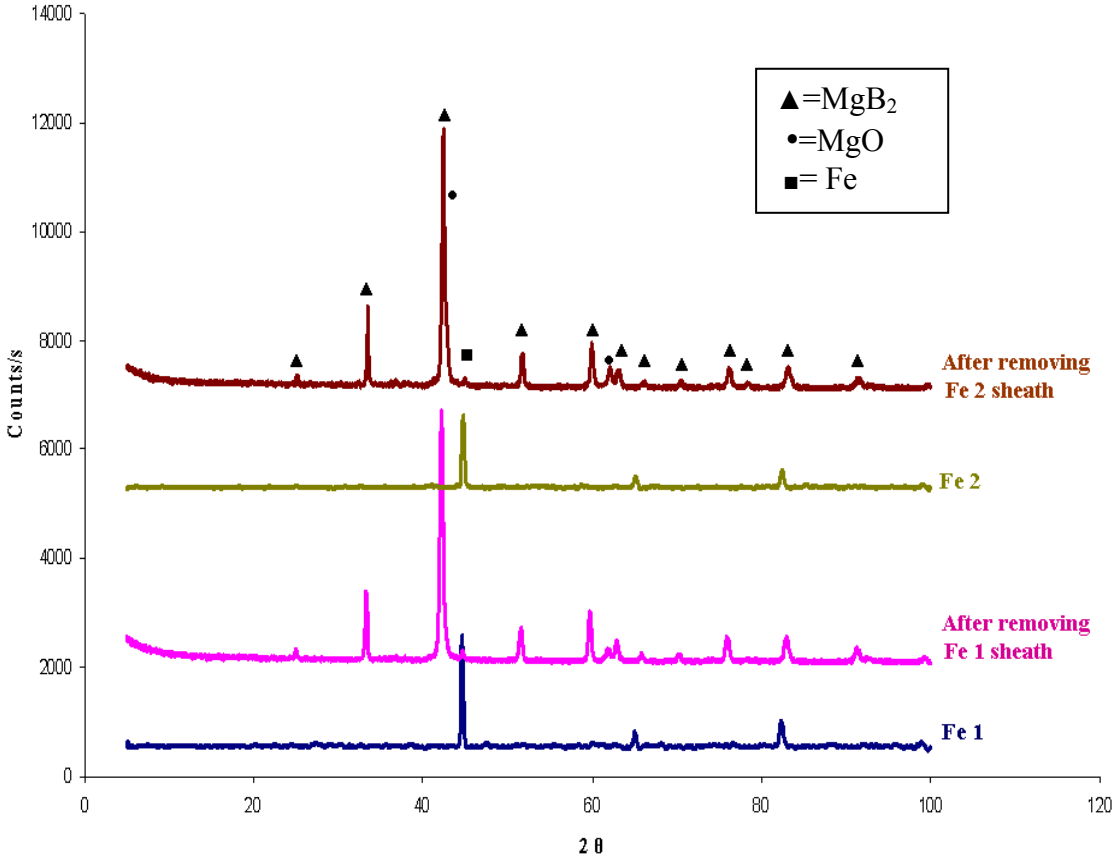

Figure 4.2. XRD Patterns of Iron Sheaths and Powders after Removing Iron Sheats

The *I-V* measurement of Fe 1 sheathed wire is shown in Figure 4.3. The I_c value of the wire was about 25 A at 4 K. This result obviously revealed that it is possible to synthesize iron sheathed MgB_2 wires with good performance. Further optimization of processing conditions such as the densification of the core and the

doping of effective pinning centers will guide to the synthesis of higher performance superconducting MgB_2/Fe 1 wires.

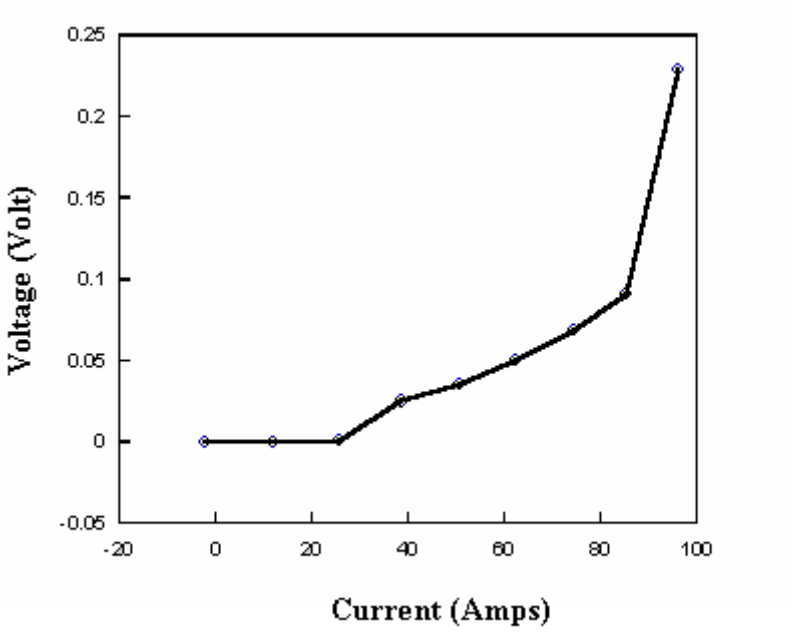

Figure 4.3. *I-V* Curve at 4 K and Self Field for MgB_2/Fe 1 Wire

Figure 4.4. shows the XRD patterns of copper sheath material and powder from the core of the wire after copper sheath was mechanically removed. It was found that, $MgCu_2$ forms instead of MgB_2 even at 700^{o}C because of Cu and Mg diffusion between Cu sheath and (Mg+2B) core. There is also amorphous boron in the core due to the loss of Mg during the formation of intemetallic alloy $MgCu_2$. No peaks of unreacted Mg were observed in any of the samples. It means that Mg was used by copper sheath for the formation of $MgCu_2$ layer.

However, Shimura reached a self field I_c of 100 A (Shimura, et al. 2004) and also Sumption obtained the critical current density of $3x10^5$ A/cm^2 for multifilamentary Cu sheathed MgB_2 wires (Sumption, et al. 2005). Although a few groups claimed that Cu sheathed conductors have high I_c and good thermal stabilization for practical applications, our results showed that Cu can not be used without a protective barrier and Fe is one of the best sheath material because of the lack of reaction between Fe and the superconducting MgB_2 material.

The *I-V* measurement of copper sheathed MgB_2 wire is shown in Figure 4.5. As it can also be seen from the *I-V* curve, copper clad MgB_2 wire could not carry current and formed a resistance. These results clearly demonstrate that copper is not feasible to

use as a sheath material and it is not really possible to synthesize Cu sheathed MgB_2 wire with good performance.

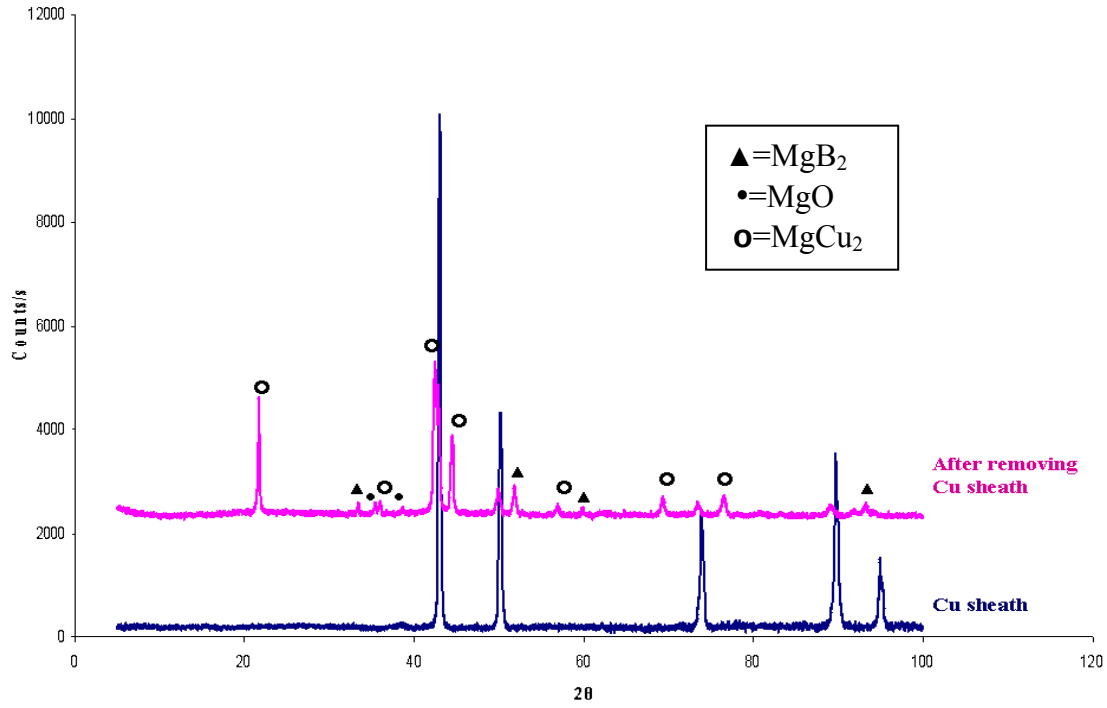

Figure 4.4. XRD Patterns of Copper Sheath and Powder from the Core of the Wire after Copper Sheath was Mechanically Removed

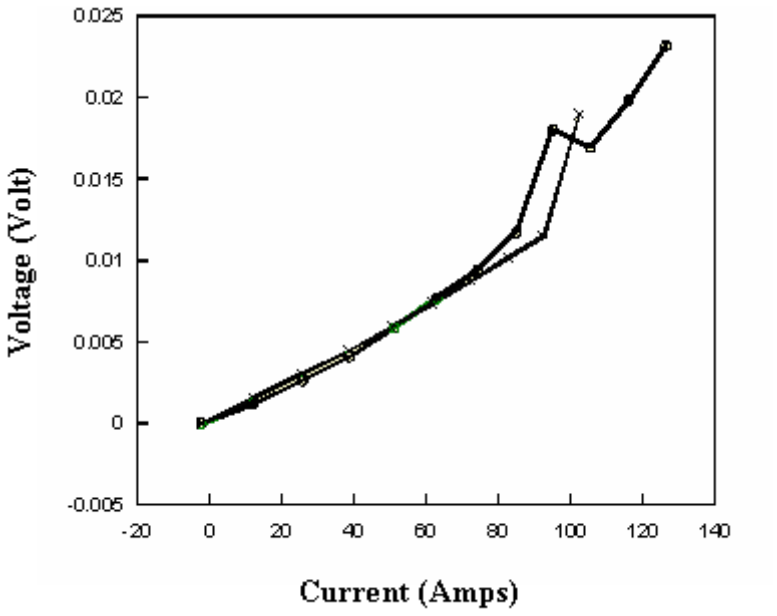

Figure 4.5. *I-V* Curve at 4 K and Self Field for MgB_2/Cu Wire

Figure 4.6. shows SEM micrographs of transverse section of annealed Fe 1, Fe 2 and Cu clad MgB_2 wires. It can be seen that a more distinct interface layer exists

between the sheath material and the superconducting core in Fe 1 and Fe 2 clad MgB_2 wires compared to Cu clad MgB_2 wires due to the strong interaction of copper sheath with Mg+2B core.

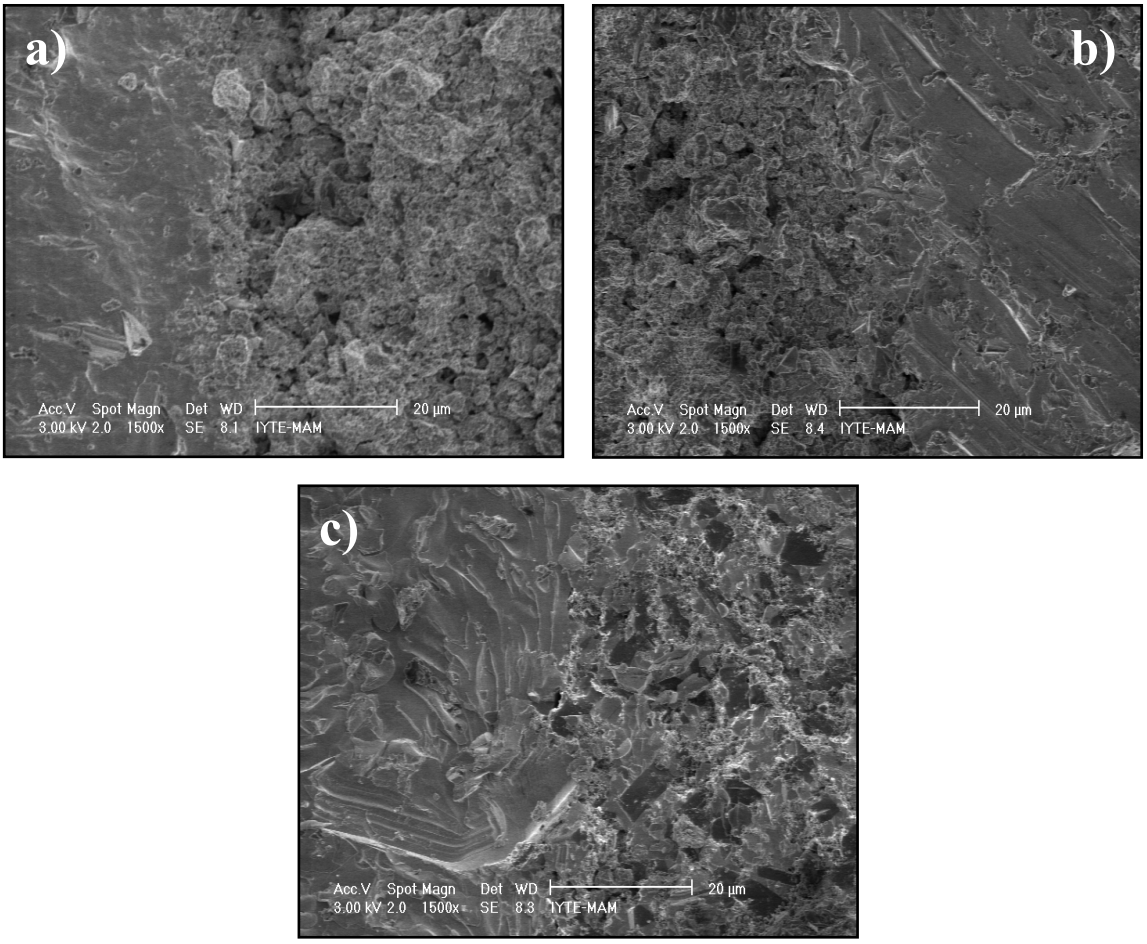

Figure 4.6. SEM Micrographs of Samples (a) the Core of the Fe 1-clad MgB_2 Wire (b) the Core of the Fe 2-clad MgB_2 Wire (c) the Core of the Cu-clad MgB_2 Wire

4.1.1.2. Effect of Annealing Temperature

Even though MgB_2 phase formation occurs at lower temperatures, suitable high temperature heat treatments are needed for providing better superconducting properties, In the case of MgB_2 the final heat treatment temperature for better properties is estimated between 650-800°C and the heat treatment is done in vacuum or oxygen protective environments (Vinod, et al. 2007). Heating of rolled sample improves the intergrain connectivity, reduces the porosity, heals the cracks formed during rolling and improves the texturing.

A plausible explanation for the effect of annealing temperature on the synthesis of superconducting MgB_2 phase is as follows. Magnesium melts at ~650°C and starts evaporating as the temperature is increased, while boron (melting point~ 2079°C) is stable at all temperatures employed for the synthesis. When the samples are prepared at temperatures as high as 950°C, Mg would evaporate quickly if the particle size is small because of larger surface to volume ratio (Aswal, et al. 2001). These results also show that the formation of MgB_2 takes place by diffusive reaction of Mg with boron.

The sintering temperature and the sintering time of MgB_2/Fe wires are given in Table 4.1. According to these literature works, wires of 50 mm in length were annealed for 30 min. at different temperatures ranging between 700°C to 850°C in Ar gas atmosphere. Effect of annealing temperature on the phase composition, microstructure features, transition temperature and critical current were investigated by using X-ray diffractometer, scanning electron microscopy with an energy dispersive spectrometer and the standard DC four probe point technique.

Sintering Temperature	***Sintering Time***	**References**
600-900°C	0.5-3h	Salama, et al. 2007
700-900°C	2h	Xu, et al. 2005
675-900°C	5min-10h	Bhatia, et al. 2004
650-850°C	2-5h	Yan, et al. 2003
745-900°C	3-32min	Wang, et al. 2001

Table 4.1. The Range of Sintering Temperature and Time for MgB_2/Fe Wires

MgB_2/Fe superconducting wires have been successfully produced by the PIT method: an in situ groove rolling technique where an Mg+2B mixture was used as a central conductor core and reacted in situ to form MgB_2. An as-rolled long Fe 1 sheathed MgB_2 square wire was flexible and uniform, and the surface was shiny and metallic. Powder XRD patterns of the samples are shown in Figure 4.7. Referring to the precursor mixture before annealing, all the peaks of the X-Ray diffraction patterns of the as-milled Mg and B powder mixture are associated with Mg, which indicates that within 3 hours of milling, Mg and B do not react to form MgB_2 phase. However, MgB_2 was the main phase in all annealed samples. Other impurity phases were MgO, Fe from sheath material, and a little unreacted Mg only in the sample at 700°C. No peaks of MgB_4 or other borides were observed in any of the samples. Although there may be some unreacted amorphous boron, these could not be detected by XRD. It indicates that the Fe 1 sheath did not react with either boron or magnesium.

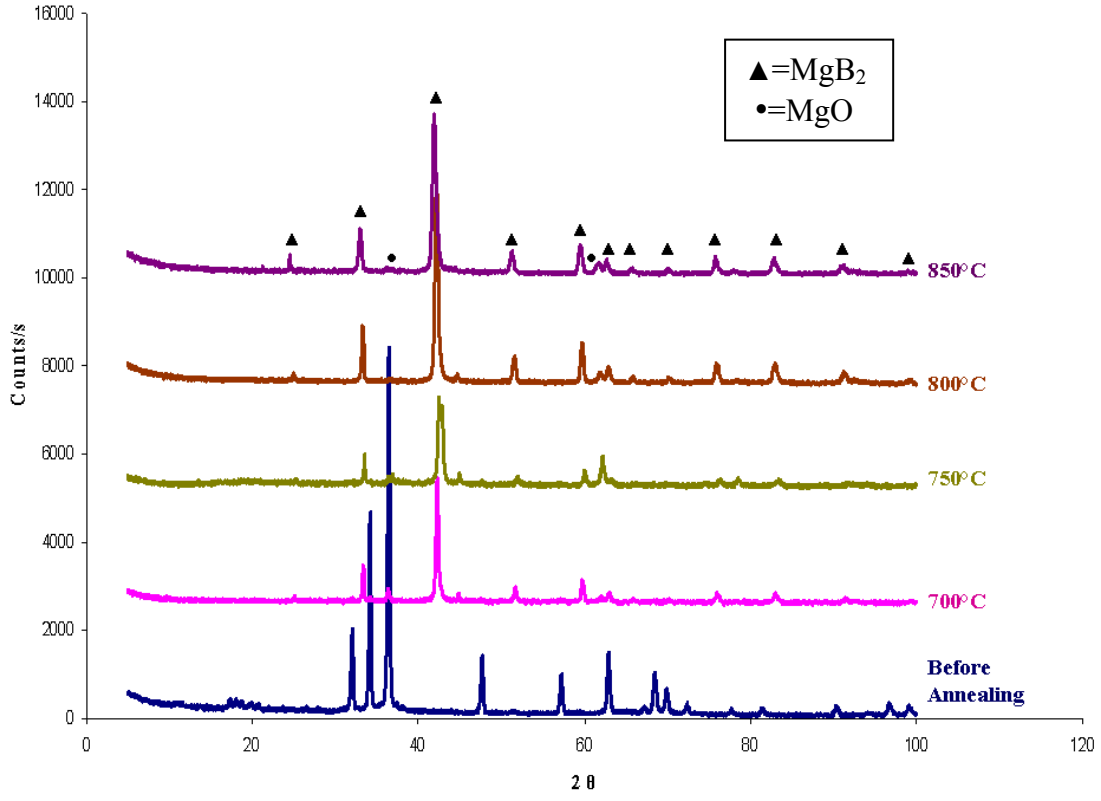

Figure 4.7. XRD Patterns of the Precursor Mg and B (AB) Powder Mixture before Annealing and MgB_2 Powders from the Core of the Fe 1 Sheathed Wire after Different Heat Treatments

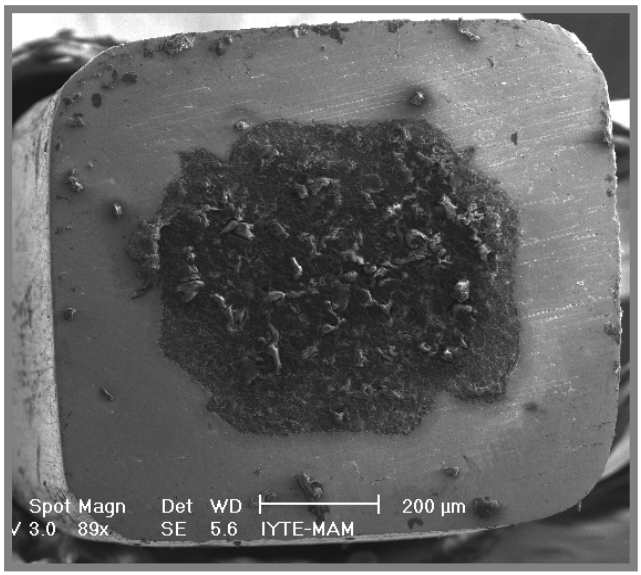

Figure 4.8. SEM Micrograph of Polished Cross Section of the Light Iron Sheathed MgB_2 Wire

Figure 4.8. shows typical SEM image of cross section of a 1 mm diameter of an annealed Fe 1 sheathed MgB_2 wire with 5% excess Mg. The diameter of the superconducting core has been measured to be about 0.6 mm from SEM micrograph. The wire has a square cross section because it is reduced by square type groove roller. A square wire with the dimensions of about 1 mm by 1 mm cross sectional area is gradually obtained. The cross sectional area of the MgB_2 core was about 0.27 mm^2, therefore the superconducting fill factor was about 27 % of the whole conductor cross section.

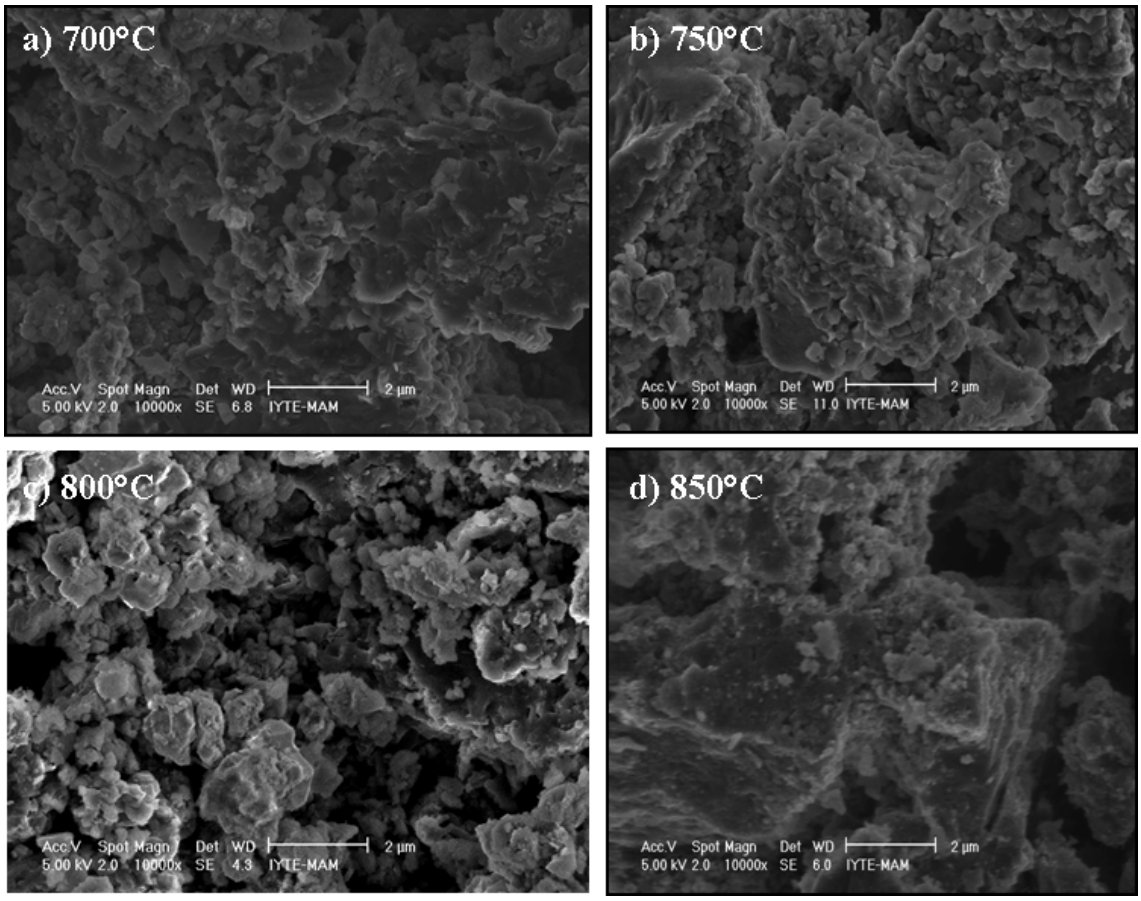

Figure 4.9. SEM Micrographs of Fe 1 Sheathed MgB_2 Wires after Annealing at Different Temperatures

The sintering process decreases the porosity and increases the connectivity between particles, therefore provides a more homogeneous structure. As shown in the SEM micrographs in Figure 4.9, while the annealing temperature increases the pores gradually close. According to this, the Tc critical transition temperature gradually increases while the annealing temperature increases. Resistivity versus temperature plot for heat treated MgB_2 wires in zero field is shown in Figure 4.10.

Short pieces of samples were cut from Fe 1 clad MgB_2 wires to measure the temperature dependent resistivity. The critical temperature of the sample sintered for 30 min. at 700°C is Tc onset= 41.554 K, and Tc zero=38.051 K. By raising the sintering temperature further, the critical temperature increases and shows a maximum around 800-850°C. Although, MgB_2 wire sintered at 850°C shows a sharp transition, it has a non-zero resistivity which is due to MgO impurity, while the others show superconducting transition with zero resistivity. Therefore; the results of XRD measurements are in agreement with the R-T measurements. Hence, we found that there is an optimal sintering temperature as 800°C. The width of the superconducting

transition, Tc onset – Tc zero was calculated as shown in Table 4.2. MgB_2 wires annealed at 800°C shows a sharper transition with a narrow width of 0.397 K, indicating the good homogeneity of the samples. Within the optimal temperature, the superconducting transition becomes sharper, Figure 4.10.c. This demonstrates that synthesis of the samples for 30 min. at 800°C is useful for enhancing the quality of MgB_2.

	Tc (K)	*Tc onset(K)*	*Tc zero(K)*	**ΔTc (K)**
700°C	39.484	41.554	38.051	3.503
750°C	39.195	40.315	38.398	1.917
800°C	39.878	40.150	39.753	0.397
850°C	40.137	40.143	39.929	0.214

Table 4.2. Transition Temperatures of the MgB_2 Wires Heat Treated for 30 min at Four Different Temperatures between 700-850°C

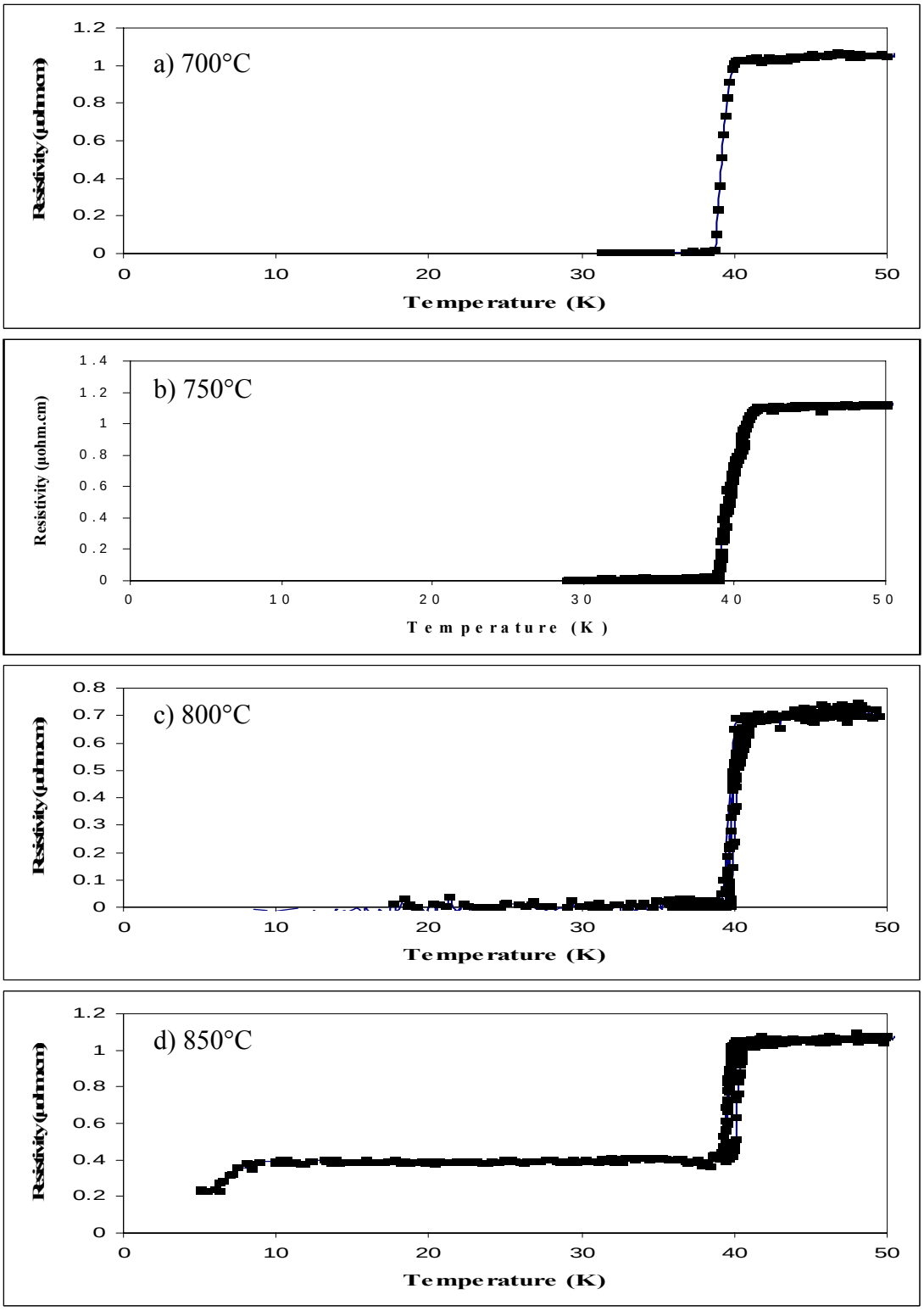

Figure 4.10. R-T Characteristics of Sintered MgB_2 Wires with Fe 1 Sheath Material at a Driven Current of 5 mA

4.1.2. Boronsan Boron used as a Precursor Boron Powder

In this part of the study, a different boron powder produced by the high temperature electolysis process of sodium borates (Yıldıran and Güler 2006) was used to investigate the effects of precursor boron powder on the reaction between Mg and B, and their influence on the superconducting properties. Boron powder from Boronsan (90% purity) was mixed with Commercial Mg powder (99.8% purity) from Alfa Aesar and homogenized by ball milling for 3 hours. Additionally, 0-5-10-15 wt% of extra Mg were added to the in-situ MgB_2 powders, in order to investigate the effect of chemical doping on the superconducting characteristics of MgB_2. The influence of heat treatment for optimum Mg/B ratio was also studied in relation to the improvement of superconducting properties.

4.1.2.1. Effect of Chemical Doping

The effect of chemical doping on superconductivity in MgB_2 compound has been studied by several groups. There are several factors that affect the cost and quality while producing MgB_2. One of these is the quality of the Mg and B elements that are used as precursor materials. Another factor is the proportions of the Mg and B to form MgB_2. Hinks worked on the effect of the different stoichiometric coefficients of Mg and B during the sintering process (Hinks, et al. 2002). In his work, Hinks formulized the excess and inadequate Mg amounts as (Mg_xB_2) $0.5 \geq x \geq 1.3$. A similar research was carried out by Ribeiro and was observed that when the Mg amount is inadequate, the phase of MgB_4 is formed (Ribeiro, et al. 2002). In both researches, the maximum transition temperatures was obtained when x=1 for Mg_xB_2. However, for MgB_2 superconductors including bulk, powders, wires, tapes and thin films, the samples are usually prepared at the temperature high above the melting point (~650°C) of Mg. It is well known that Mg is highly volatile at high temperatures. Therefore, it is possible that Mg is easily lost during the preparing process of the sample. That is, the prepared samples usually have Mg deficiency; hence, to account for such a loss it would be necessary to increase the amount of Mg than in the stoichiometric ratio, prior to the heat treatment (Xiao, et al. 2003). Vinod also observed that the reactivity of Mg with B decreases significantly due to the reduction in diffusion of particles across MgB_2 layer (Vinod, et al. 2007).

Examination of the micrographs presented in Jiang's work (Jiang and Kumakura 2007) for the undoped samples with Mg/B variation shows that the Mg deficient samples demonstrate a microstucture composed of a loose network of connected grain clusters. As the Mg level is increased, a denser network is observed. Ma and his friends investigated undoped MgB_2 and have noted a microstructure similar to that seen in Jiang's Mg deficient samples. No general opinion has been reached on the effect of excess Mg on the superconducting properties of PIT MgB_2 wires. Literature works have differences in purity, particle size, the use of MgB_2 instead of elemental Mg as the Mg source, and the possible perturbing effect of MgO formation (Susner, et al. 2007).

In order to study the effect of magnesium stoichiometry on the superconducting properties of Mg doped MgB_2 samples, with a nominal composition of $Mg_{(1+x)}B_2$ (x = 0, 0.05, 0.10, and 0.15), have been synthesized by solid state reaction. Figure 4.11. presents powder X-ray diffraction patterns of the undoped and Mg-doped samples.

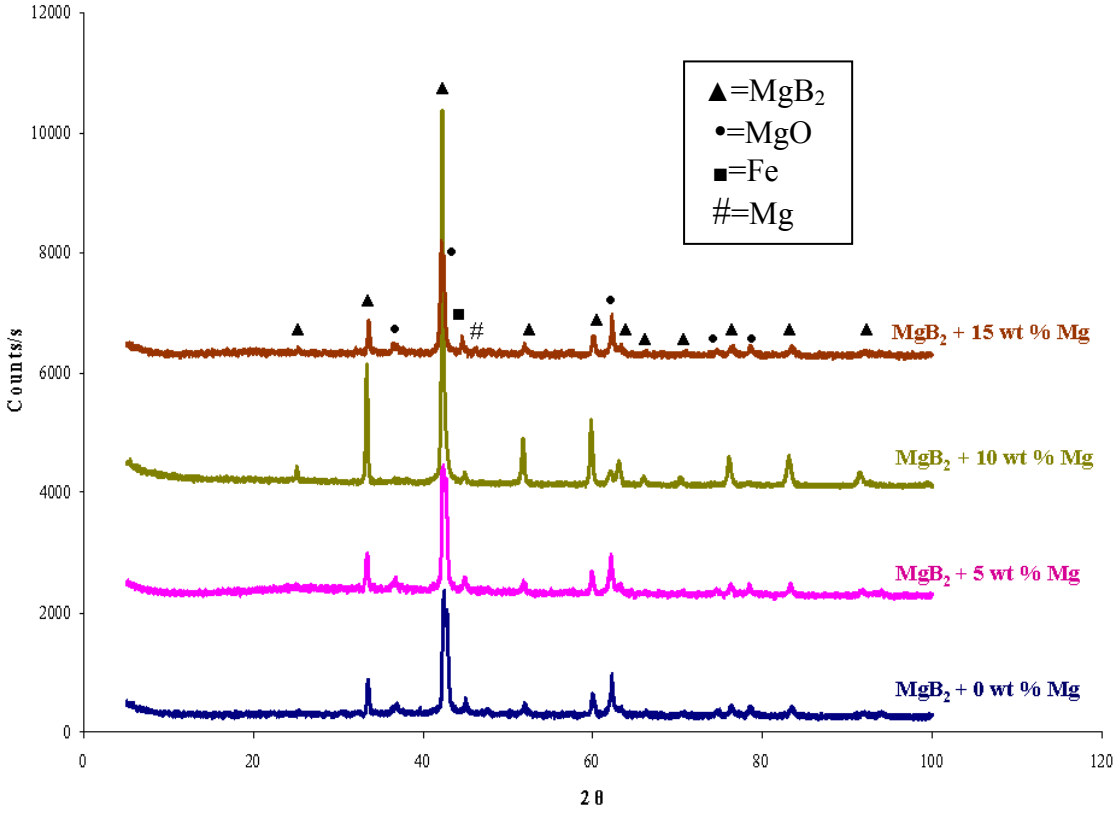

Figure 4.11. XRD Patterns of the Undoped and Mg-doped Samples Heat Treated at 750°C for 30 Minutes

The spectra of MgB_2 phase were obtained as expected, though some impurities were observed. In all cases the lines seen at 2θ = 44.671° is associated with Fe (marked with ■) from the sheath material during mechanically removing the powder. From the spectra, it can be seen that the strongest peak of MgB_2 (2θ = 42.412°) broadens at 0-5-15 wt % Mg doped MgB_2 samples due to considerable amount of MgO formation, whereas 10 wt % Mg doped sample has sharper MgB_2 peak without MgO impurity. The broadening is due to the overlapping of the strongest peak of MgB_2 and MgO (2θ = 42.824°). The reason for the formation of MgO could be attributed both to the trapped oxygen in the powder and also to the precursor boron powder which is produced by electrolysis of sodium borates ($Na_2B_4O_7.5H_2O$). The precursor boron powder has been analyzed by XRD and it is shown that it consists of sodium borate known as tincalconite, and unidentified impurities (Figure 4.12.). Distinctively, MgO peak at 2θ value of 62.167 can be compared with MgB_2 peak at 2θ value of 63.173. The comparison shows that the MgB_2 peak has higher intensity than peak than MgO peak, when x = 0.10 in $Mg_{(1+x)}B_2$ sample. There is no proportional change with respect to the amount of Mg doping in our samples. 0-5-15 wt % Mg doped MgB_2 samples are similar to each other except weak MgB_2 peak at 2θ value of 25.266° and weak diffraction line at 2θ value of 47.807° associated with unreacted Mg for 15 wt % Mg doped sample. That is, 10 wt % extra Mg addition was seen to be beneficial compared to the stoichiometric MgB_2.

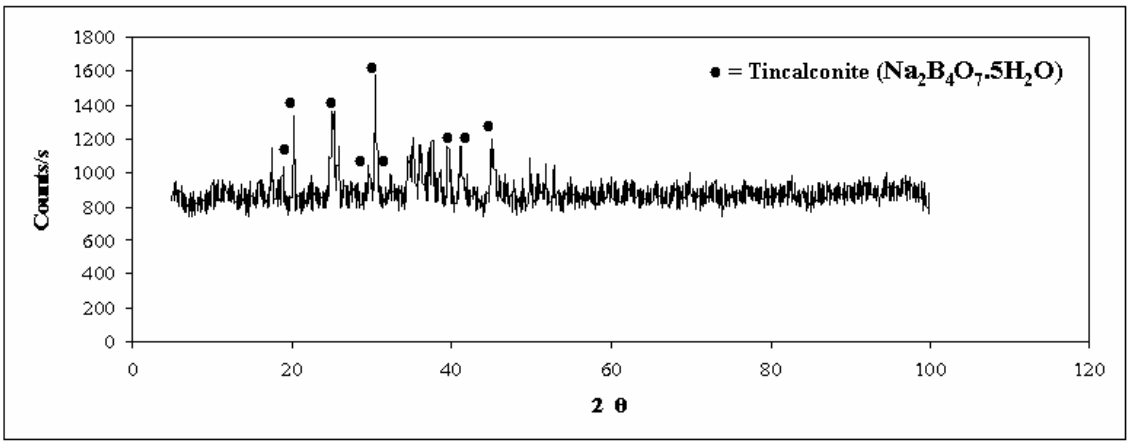

Figure 4.12. XRD Pattern of Boronsan Boron Powder

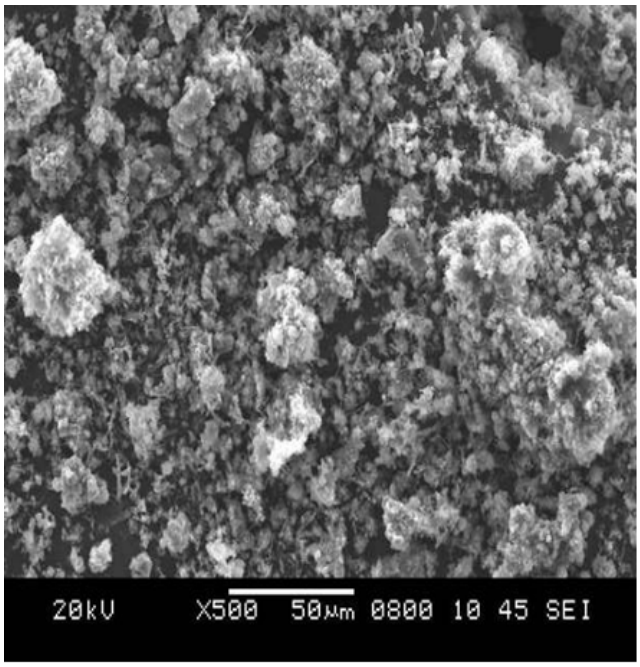

Component	Conc.		
O	3.995	wt.%	
Ni	0.141	wt.%	
Si	0.032	wt.%	
Ca	0.080	wt.%	
Zn	0.136	wt.%	
Cu	0.257	wt.%	
Cr	0.682	wt.%	
Fe	1.232	wt.%	
B	92.873	wt.%	
Na	0.571	wt.%	
	100.000	wt.%	Total

Elt.	Line	Intensity (c/s)	Error 2-sig	Conc		
B	Ka	22.36	1.206	92.873	wt.%	
O	Ka	10.46	0.800	3.995	wt.%	
Na	Ka	21.93	1.112	0.571	wt.%	
Si	Ka	2.08	0.785	0.032	wt.%	
Ca	Ka	3.51	0.707	0.080	wt.%	
Cr	Ka	18.27	1.003	0.682	wt.%	
Fe	Ka	23.90	1.082	1.232	wt.%	
Ni	Ka	1.99	0.473	0.141	wt.%	
Cu	Ka	2.83	0.508	0.257	wt.%	
Zn	Ka	1.22	0.451	0.136	wt.%	
				100.000	wt.%	Total

Figure 4.13. SEM Micrograph and EDX Results of Boronsan Boron Powder

4.1.2.2. Effect of the Annealing Temperature

Reaction between Mg and B starts at temperatures well below the melting point of Mg (Cui, et al. 2004). As the annealing temperature increases Mg starts to react with B to form MgB_2. The reaction between Mg and B powders starts at the Mg-B interface and a layer of MgB_2 forms at the interface (Shi, et al. 2007, Yan, et al. 2007, Liu, et al. 2007). At the reaction temperature Mg melts but remains as globules and can be considered as particles in liquid phase. Mg and B particles diffuse across the formed MgB_2 layers and MgB_2 grain grows, until the growth is pinned chiefly by pores.

Figure 4.13. presents the powder XRD spectra of 10 wt % Mg doped MgB_2 samples synthesized for 30 minutes at four different temperatures: 700, 750, 800 and 850°C. This temperature region corresponds to the formation of MgB_2 phase. It is observed that the sample at 700°C contains unreacted Mg, whereas traces of Mg are not visible in the XRD patterns of the 750, 800 and 850°C sample. However, the amount of unidentified impurity phases (marked with ?) increase with an increase in synthesis temperature.

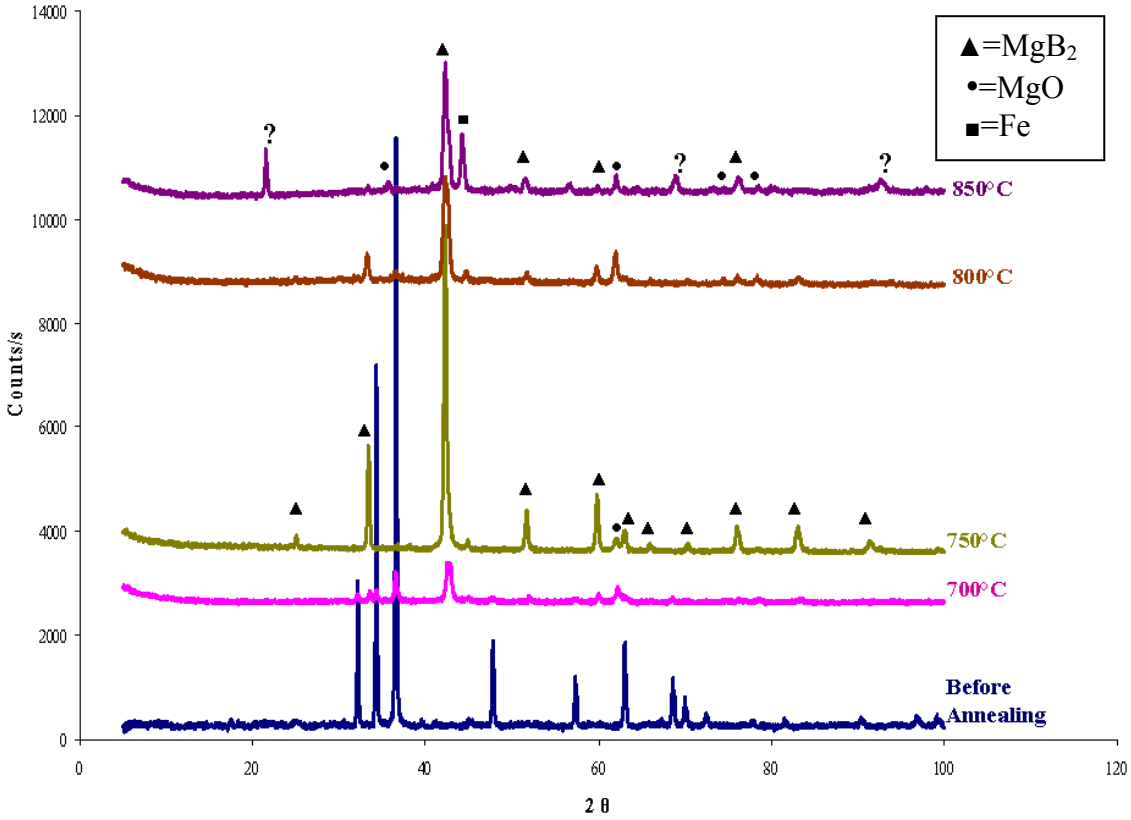

Figure 4.14. XRD Patterns of the Precursor Mg and B (Boronsan) Powder Mixture before Annealing and MgB_2 Powders from the Core of the Fe Sheathed Wire after Different Heat Treatments

The iron coming from the sheath material is clearly identified when the sample is heated to 850°C but iron did not react with B or Mg. Magnesium diboride peak at 2θ value of 25.266° can only be observed at 750°C annealing but not in the others. In addition, it is seen that the strongest peak in MgB_2 (2θ = 42.412°) broadens as the samples are heated to 700-800-850°C and considerable amount of MgO is formed, sample at 750°C has a sharp MgB_2 peak without MgO impurity. The reason of broadening is due to the overlapping of the strongest peak of MgB_2 with MgO (2θ = 42.824°). When we compare the peaks of MgO at 2θ = 62.167° and MgB_2 at 2θ = 63.173°, we can see MgB_2 peak only at 750°C annealing. The spectra at 700-800-850°C show only MgO peak but no MgB_2 peak. Although we could not observe a linear change, we decided that heating at 750°C is the most suitable temperature for the formation of MgB_2 phase.

In contrast to the common practice of sintering for several hours, our results show that there is no need for long time heat treatment in the fabrication of Fe-clad MgB_2 wires.

The *I-V* measurement of Fe sheathed wire is shown in Figure 4.14. The I_c value of the wire was measured as 13 A at 4 K. The capacity of these wires for current loading is lower compared to the capacity of wires made using AB Boron. We think that the reason for this decrease of current is due to the formation of unwanted MgO and some unidentified impurities which prevents for the formation of single MgB_2 phase.

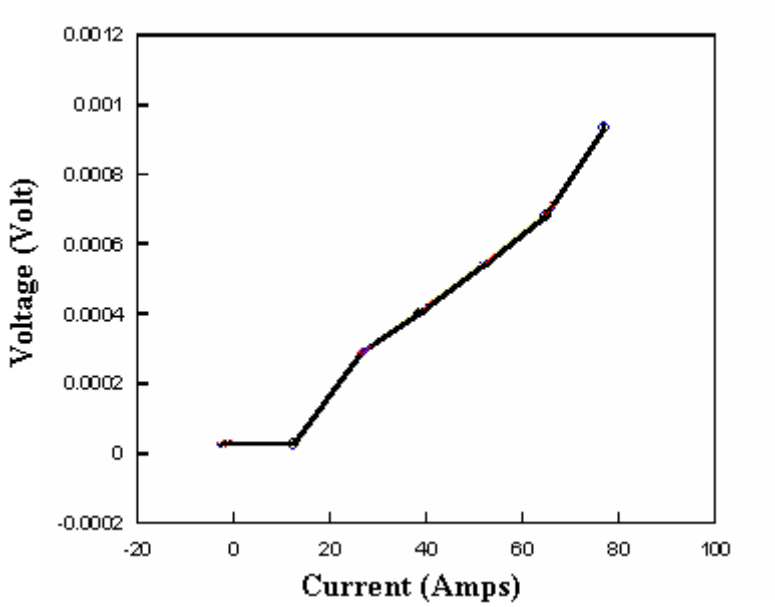

Figure 4.15. *I-V* Curve at 4 K and Self Field for MgB_2/Fe Wire

Resistivity versus temperature plot for the MgB_2/Fe wire which is heat treated under conventional conditions (750°C for 30 min) in zero field is shown in Figure 4.15. It shows a broader transition with non-zero resistivity transition temperature of 24 K. This value is much lower than the ideal value of 39 K.

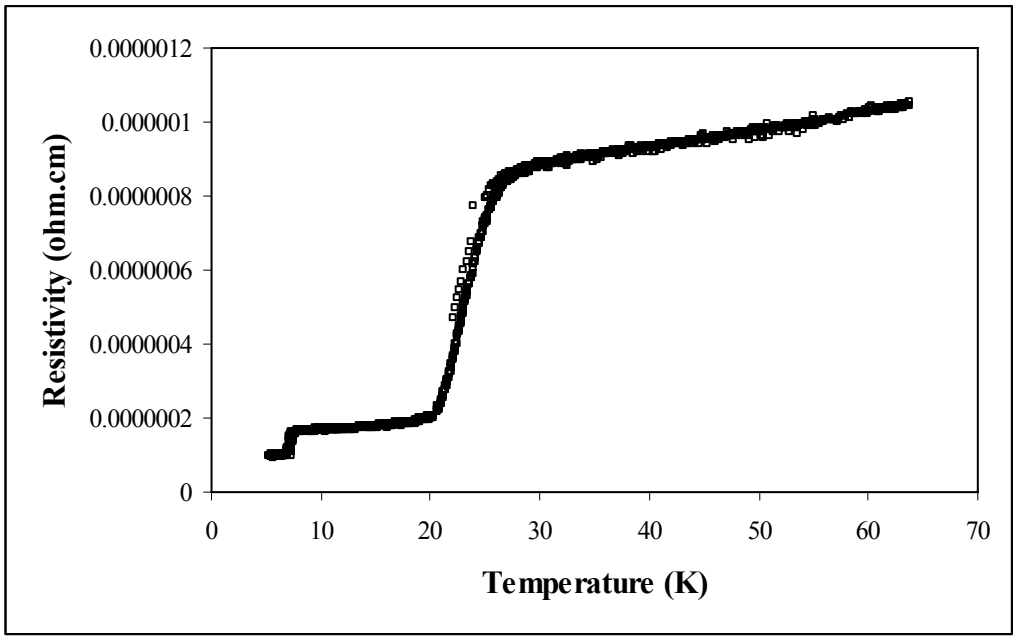

Figure 4.16. R-T Characteristics of MgB_2/Fe Wire Sintered under 750°C at a Driven Current of 5 mA

Voltage-current measurements and also resistivity-temperature measurements are consistent with the results of XRD analysis. We think that both X-ray line and transition broadening are possible effects of MgO and some unidentified impurities on the superconducting properties of MgB_2.

4.2. Four-Filament MgB_2 Wires Results

MgB_2 superconductors have a variety of commercial applications: magnetic resonance imaging, fault current limiters, transformers, motors, generators, adiabatic demagnetization refrigerators, magnetic separation, magnetic levitation, superconducting magnetic energy storage, and high energy physics applications (Tomsic, et al. 2007)

Significant processes have been made since 2001 on the development of long-length MgB_2 superconductor wires. Presently, the future is promising for MgB_2 superconductors, as there are several ongoing demonstration projects that are directed toward commercial applications.

We tried to fabricate in situ MgB_2 wire 200 m long in laboratory conditions, and successfully produced four filament MgB_2/Cu wire by the PIT method. Four pieces of

monofilament copper clad wire, each about 4 m in length and 2 mm in diameter, were inserted into a copper tube that had 5 mm inner and 8 mm outer diameter. Groove rolling process was repeated to reduce the diameter of four filament wire to about 1 mm in outer diameter. The inner filaments have final diameters of about 0.1 mm. Figure 4.16. shows a typical wire cross section of the four filament wire fabricated at İzmir Institute of Technology (Iz Tech).

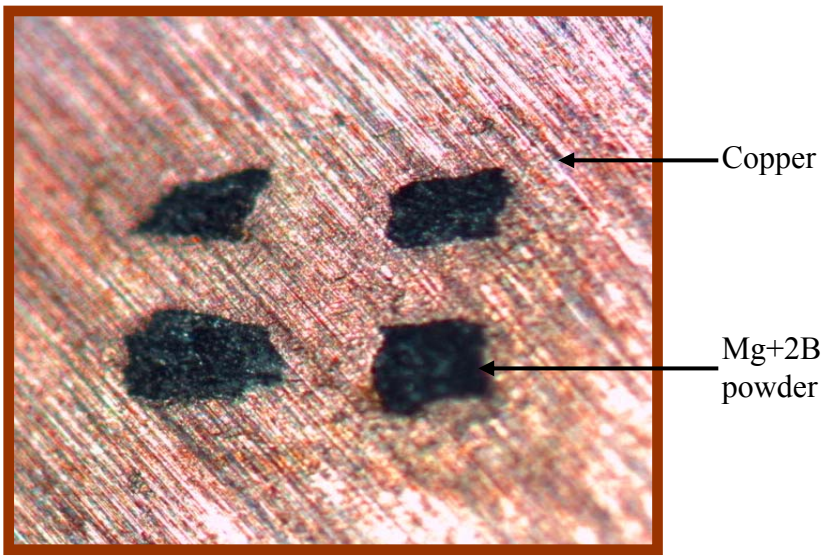

Figure 4.17. Cross Section of a Typical Four Filament MgB_2/Cu Wire

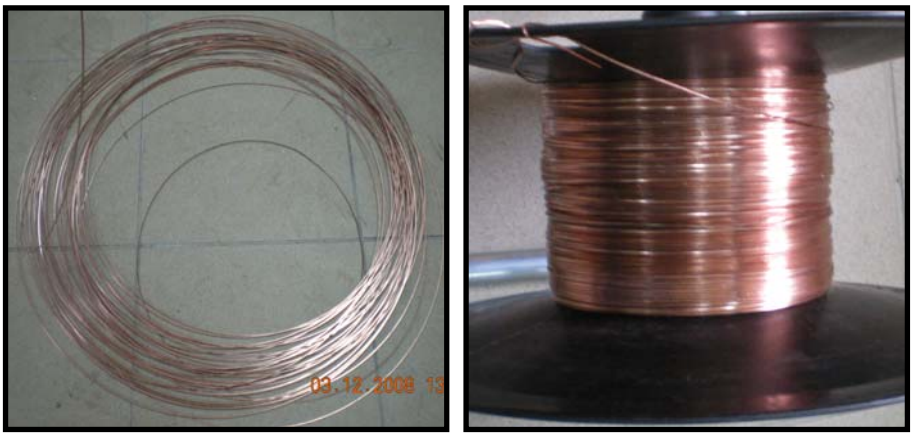

Figure 4.18. In situ Four Filament MgB_2/Cu Wire 200 m Long

Copper tubes were used as cheap and easily available sheath material to check whether such wires can be fabricated under laboratory conditions. However, it was found that copper tubes were not suitable as sheath material. Thus, wires were prepared with iron sheaths, afterwards heat treatment was applied to these wires and their superconducting properties were investigated.

Figure 4.19. MgB_2/Fe Wire Produced by in situ PIT Method

CHAPTER 5

CONCLUSION

Magnesium diboride has a high critical temperature and current density and low cost. This gives advantage to these materials in terms of applicability among other superconductors. MgB_2 offers a higher operating temperature (20 K) in the current technology compared to Nb-based superconductors (4.2 K). Therefore, production of MgB_2 wires has great importance in scientific and industrial applications.

MgB_2 is in powder form as a precursor material hence, this material has to be transformed into wire and tape before using in technological applications. The most common method to produce wire from fragile powders is the powder in tube (PIT) method.

In this study, investigation of the effects of precursor boron powder on the reaction between Mg and B, and their influence on the superconducting properties were aimed. The importance of B for the MgB_2 production is clear, and this makes our study even more important because Turkey has the biggest boron sources in the world. We have synthesized MgB_2 wires with boron powders of different purities. The effect of B powder purity on the current and critical transition temperature of there superconductors is definitely important. Impurities in boron powder can suppress both current values and critical transition temperature.

In the first part of the study, MgB_2 synthesis using commercial magnesium powder and AB boron powder (95-97% purity), and its microstructural and electrical characterization was aimed. The possibility of using commercial soft copper tubes as a sheath material for MgB_2 wires fabricated by in situ PIT method and comparison of their performance with those of the wires stacked in iron sheaths were investigated. Unreacted (5 wt % Mg doped Mg+2B) wires with a Cu and Fe sheath were prepared. Short samples from Cu and Fe clad unreacted (Mg+2B) wires were heat treated for 30 min at four different temperatures between 700-850°C in Ar gas atmosphere.

The powder in the cores of Cu and Fe sheath were mechanically removed and microstructural studies using XRD and SEM were carried. It was found that, in Cu clad cores considerable amount of $MgCu_2$ forms instead of MgB_2 even at 700^oC because of Cu and Mg diffusion between Cu sheath and (Mg+2B) core, while on Fe clad cores, the

major phase is MgB_2 with minor MgO constituent. R-T and V-I measurements were performed to investigate the effect of Cu and Fe sheath on critical temperature (T_c) and critical current (I_c) of in-situ MgB_2 wires. The transition temperatures of Fe clad wires are between 39 K and 40 K, whereas any transition temperature was not observed at Cu clad wires. In addition, the I_c value of the Fe clad wire was about 25 A at 4 K, while the copper clad MgB_2 wire could not carry any current and formed a resistance. Our results showed that Fe is still one of the best sheath materials because of the lack of reaction between Fe and the superconducting MgB_2 material.

In order to investigate the effect of the annealing temperature, unreacted (5 wt % Mg doped Mg+2B) wires with a light coloured iron (Fe 1) sheath were heat treated for 30 min. at temperatures from 700 to 850°C. XRD patterns of the MgB_2 powders from the core of the Fe 1 sheathed wire after different heat treatments showed that sample at 800°C has a sharp MgB_2 peak without MgO impurity. By raising the sintering temperature further, the critical temperature increases and shows a maximum around 800-850°C. Although, MgB_2 wire sintered at 850°C shows a sharp transition at 40 K, it has a non-zero resistivity, while the others show superconducting transition with zero resistivity. Therefore; the results of XRD measurements are in agreement with the R-T measurements. Hence, we concluded the optimal sintering temperature as 800°C.

In the second part of our study, MgB_2 synthesis using commercial magnesium and Boronsan boron (90% purity) which is produced in Turkey by the high temperature electolysis of sodium borates was tried. Additionally, 0-5-10-15 wt% of extra Mg were added to the in-situ MgB_2 powders, in order to investigate the effect of chemical doping on the superconducting characteristics of MgB_2. The influence of heat treatment at optimum Mg/B ratio was also studied in relation to the improvement of superconducting properties.

Mg doped MgB_2 samples, with a nominal composition of $Mg_{(1+x)}B_2$ (x = 0, 0.05, 0.10, and 0.15) have been synthesized by solid state reaction to investigate the effect of magnesium stoichiometry on the superconducting properties. X-ray diffraction patterns of the undoped and Mg-doped samples were studied. Samples with $Mg_{(1+x)}B_2$ (x = 0.10) showed higher intensity MgB_2 peak than MgO peak. In these wires, 0-5-15 wt % Mg doped MgB_2 samples demonstrated similar results except weak MgB_2 peak at 2θ value of 25.266°. Additionally, it was seen that weak diffraction line at 2θ value of 47.807° associated with unreacted Mg for 15 wt % Mg doped sample was present. As a result,

10 wt % extra Mg addition to the stoichiometric MgB_2 was found to be the most suitable composition.

10 wt % Mg doped MgB_2 samples have been sintered for 30 minutes at four different temperatures: 700, 750, 800 and 850°C. XRD spectra of the MgB_2 samples showed that heating at 750°C is the most suitable temperature for the formation of MgB_2 phase. MgB_2/Fe wire shows a broader transition with non-zero resistivity transition temperature of 24 K. This value is much lower than the ideal value of 39 K. In additon, the I_c value of the wire was measured as 13 A at 4 K. The capacity of these wires for current loading is lower compared to the capacity of wires made using AB Boron (I_c =25 A). We think that the reason for this decrease of current is due to the formation of unwanted MgO and some unidentified impurities which prevent the formation of single MgB_2 phase. The reason for the formation of MgO might be attributed both to the trapped oxygen during heat treatment and mainly to the precursor boron powder which is produced by electrolysis of sodium borates ($Na_2B_4O_7.5H_2O$).

In the third part of our study, we have proved the productibility of a four filament MgB_2/Cu wire 200 m long in laboratory conditions. The next step is to produce long length MgB_2 wire using Fe sheath for industrial applications.

The study can be summarized as follows:

– The most important factor that prevents the formation of MgB_2 phase is the sheath material. According to our results, although copper is a cheap and flexible material which is easily available, copper reacts with Mg and turns into $MgCu_2$ phase. Therefore; studies should be concentrated on the production of superconducting wires with Fe sheaths and on increasing their current carrying capacities.

– Purity of starting materials is very important, thus, oxygen presence should be avoided throughout the procedures.

– Although boron powder obtained from Boronsan did not give satisfactory results, its purity can be improved by soxhlet extraction or zone refining techniques.

– Further optimization of processing conditions such as the densification of the core and the doping of effective pinning centers will guide to the synthesis of higher performance superconducting MgB_2/Fe wires.

REFERENCES

Abrikosov, A.A. 1957. On the Magnetic Properties of the Second Group. *Soviet Physics JETP* 5:1174-1182.

Ahoranta, M., Lehtonen, J. and Kováč, P. 2004. Feasibility of Iron-Sheathed MgB_2 Wires for Magnet Applications. *Physica C* 400:89-96.

Aksan, M.A., Güldeste, A., Balcı, Y. and Yakıncı, M.E. 2006. Degradation of Superconducting Properties in MgB_2 by Cu Addition. *Solid State Communications* 137: 320.

Aswal, D.K., Sen, S., Singh, A., Chandrasekhar Rao, T.V., Vyas, J.C:, Gupta, L.C., Gupta, S.K. and Sahni, V.C. 2001. Synthesis and Characterization of MgB_2 Superconductor. *Physica C* 363:149-154.

Bardeen, J., Cooper, L.N., and Schreiffer, J.R. 1957. Theory of Superconductivity. *Physical Review* 108:1175-1204.

Balkan, Naci and Erol, Ayşe. 2005. *Çevremizdeki Fizik: Süperiletkenler.* Tübitak Popüler Bilim Kitapları.

Baudis, U. and Fichte, R. 2002. *Boron and Boron Alloys-Boron* Germany: Ullmann's Encyclopedia of Industrial Chemistry, Sixth Edition.

Baudis, U. and Fichte, R. 2002. *Boron and Boron Alloys-Structure and Polymorphism.* Germany: Ullmann's Encyclopedia of Industrial Chemistry, Sixth Edition.

Baudis, U. and Fichte, R. 2002. *Boron and Boron Alloys-Physical Properties.* Germany: Ullmann's Encyclopedia of Industrial Chemistry, Sixth Edition.

Baykal, Elif D. 2003. Hidrotermal ve Mikrodalga Enerjiyle, Lityum İçeren Boratlı Fosfatlı Bileşiklerin Sentezlenmesi, Kristal Yapı ve Termokimyasal Özelliklerinin İncelenmesi. *Balıkesir University thesis of M.Sc*.

Bednorz, G. and Müller, K.A. 1986. Possible High Tc Superconductivity in the Ba-La-Cu System. *Z.Phys.B* 64:189-197.

Bhatia, M., Sumption, M.D., Tomsic, M. and Collings, E.W. 2004. Influence of Heat Treatment Schedules on the Transport Current Densities of Long and Short Segments of Superconducting MgB_2 Wire. *Physica C* 407:153-159.

Bhatia, M., Sumption, M.D., Tomsic, M. and Collings, E.W. 2004. Influence of Heat Treatment Schedules on Magnetic Critical Current Density and Phase Formation in Bulk Superconducting MgB_2. *Physica C* 415:158-162.

Brotherton, Robert J. and C. Joseph Weber, eds. 2002. *Boron Compounds-Boron Halides.* Germany: Ullmann's Encyclopedia of Industrial Chemistry, Sixth Edition.

Bu, S.D., Kim, D.M., Choi, J.H., Giencke, J., Patnaik, S., Cooley, L., Hellstrom, E.E., Larbalestier, D.C., Eom, C.B., Lettieri, J., Schlom, D.G., Tian, W. and Pan, X.Q. 2002. Synthesis and Properties of C-Axis Oriented Epitaxial MgB_2 Thin Films. *Condensed Matter* 0204004.

Cambel, V., Fedor, J., Gregušová, D., Kováč, P. and Hušek, I. 2005. Large-Scale High-Resolution Scanning Microscope Used for MgB_2 Filament Characterization. *Superconductor Science and Technology* 18:417-421.

Canfield, P.C., Finnemore, D.K., Budko, S.L., Ostenson, J.E., Lapertot, G., Cunningham, C.E. and Petrovic, C. 2001. Superconductivity in Dense MgB_2 Wires. *Physical Review Letters* 86:2423.

Cantoni, M., Schilling, Nissen, H.U., and Ott, H.R. 1993. Characterisation of Superconducting Hg-Ba-Ca-Cu-Oxides. Structural and Physical Aspects. *Physica C-Superconductivity and Its Applications* 215(1-2):11-18.

Cardwell, David A. and Ginley, David S. 2003. *Hand Book of Superconducting Materials* 1:1050. Great Britain: *CRC Press*.

Cimberle, M.R., Novak, M. Manfrinetti, P. and Palenzona A. 2002. Magnetic Characterization of Sintered MgB_2 Samples: Effect of Substitution or 'Doping' with Li, Al and Si. *Superconductor Science and Technology* 15(1):43-47.

Collings, E.W., Lee, E., Sumption, M.D., Tomsic, M., Wang, X.L., Soltanian, S. and Dou, S.X. 2003. Continuous and Batch-Processed MgB_2/Fe Strands-Transport and Magnetic Properties. *Physica C* 386:555-559.

Cueilleron, J. 1944. *Ann. Chim.* 19:459. Germany: Ullmann's Encyclopedia of Industrial Chemistry, Sixth Edition.

Cueilleron, J. and Thevenot, F. 1977. Chemical Properties of Boron," in V. I. Matkovich (ed.): Boron and Refractory Borides. *Springer Verlag* 203–211.

Cui, C., Liu, D., Shen, Y., Sun, J., Mang, F., Wang, R., Liu, S., Greer, A., Chen, S. Glowacki, B. 2004. Nanoparticles of the Superductor MgB_2: Structural Characterization and *in situ* Study of Synthesis Kinetics. *Acta Materialia* 52:5757-5760.

Çeçen, D. 1969. Bor Cevherleri ve Bor'un Çağımız ve Gelecekteki Önemi, *Madencilik*, *M.M.O. Press* 8:10-18.

Dai, P., Chakoumakos, B.C., Sun, G.F, Wong, K.W., Xin, Y., and Lu, D.F. 1995. Synthesis and Neutron Powder Diffraction Study of the Superconductor $HgBa_2Ca_2Cu_3O_{8+d}$ by Tl Substitution. *Physica C-Superconductivity and Its Applications* 243(3-4):201-206.

Dancer, C.E.P., Cullen, F.L., Todd, R.I. and Grovenor, R.M. 2005. How can we Quantify Magnesium Oxide Content in Magnesium Diboride Using X-Ray Diffraction? *University of Oxford.*

Dancer, C.E.P., Bevan, A., Mikheenko, P., Abell, J.S., Todd, R.I. and Grovenor, R.M. 2005. Does Magnesium Diboride Sinter? *University of Oxford.*

Dou, X., Horvath, J., Soltanian, S., Wang, X.L., Qin, M.J., Zhou, S.H., Liu, H.K. and Munroe, P.G., 2003. *IEEE Transactions on Applied Superconductivity* 13:3199.

Dunand, D.C. 2001. Synthesis of Superconducting Mg/MgB_2 Composites. *Applied Physics Letters* 79:4186.

Eğilmez, M. 2004. Electrical, Microstructural and Mechanical Properties of MgB_2/Mg Metal Matrix Composites. *İzmir Institute of Technology thesis of M.Sc.*

Eisterer, M., Glowacki, B.A., Weber, H.W., Greenwood, L.R. and Majoros, M. 2002 Enhanced Transport Currents in Cu-Sheathed MgB_2 Wires. *Superconductor Science and Technology* 15:1088-1091.

Eom, C.B., Lee, M.K., Choi, J.H., Belenky, L., Song, X., Cooley, L.D., Naus, M.T., Patnaik, S., Jiang, J., Rikel, M., Polyanskii, A., Gurevich, A., Cai, X.Y., Bu, S.D., Babcock, S.E., Hellstrom, E.E., Labalestier, D.C., Rogado, N., Regan, K.A., Hayward, M.A., He, T., Slusky, J.S., Inumaru, K., Haas, M.K. and Cava, R.J. 2001. High Critical Current Density and Enhanced Irreversibility Field in Superconducting MgB_2 Thin Films. *Nature* 411:558.

Encyclopædia Britannica. 2008. http://www.britannica.com/ebc/art2263/Magnetization. (accessed April 12, 2008).

Evcin, A. 2007. *Bor Teknolojisi*. http://www.kimmuh.com/evcin/bor/bor1.pdf. (accessed August 20, 2006).

Feng, Y., Zhao, Y., Sun, Y.P., Liu, F.C., Fu, B.Q., Zhou, L., Cheng, C.H., Loshizuka, N. and Murakami, M. 2001. Improvement of Critical Current Density in MgB_2 Superconductors by Zr Doping at Ambient Pressure. *Applied Physical Letters* 79:3983.

Feng, Y., Yan, G., Zhao, Y., Wu, X.J., Pradhan, A.K., Zhang, X., Liu, C.F., Liu, X.H. and Zhou, L. 2003. High Critical Current Density in MgB_2/Fe Wires. *Superconductor Science and Technology* 16:682.

Feng, Q., Chen, C., Xu, J., Kong, L., Chen, X., Wang, Y., Zhang, Y. and Gao, Z. 2004. Study on the Formation of MgB_2 Phase. *Physica C* 411:41-46.

Flukiger, R., Suo, H.L., Musolino, N., Beneduce, C., Toulemonde, P., Lezza, P. 2003. Superconducting Properties of MgB_2 Tapes and Wires. *Physica C* 385:286-305.

Fu B.Q., Feng Y., Yan G., Liu C.F., Zhou L., Cao L.Z., Ruan K.Q. and Li X.G. 2003. High Transport Critical Current in MgB_2/Fe Wire by *in situ* Powder-in-Tube Process. *Physica C 392***:**1035.

Gencer, A., Okur, S., Kılıç, A. and Güçlü, N., 2005. Low-Field Behavior and Effect of Ti-Adding in the Superconductor MgB_2/Cu Wires. *IEEE Transactions on Applied Superconductivity* 1051:8223.

Ginzburg, V.L. and Landau, L.D. 1950. On the theory of Superconductivity. *Zhurnal Eksperimental' noi I Teoreticheskoi Fiziki*, 20:1064-1082.

Giunchi, G., Ceresara, S., Ripamonti, G., DiZenobio, A., Rossi, S., Chiarelli, S., Spadoni, M., Wesche, R., Bruzzone, P.L. 2002. High Performance New MgB_2 Superconducting Hollow Wires. *Condensed Matter* 0207488.

Glowacki, B.A., Majoros, M., Vickers, M., Evetts, J.E., Shi, Y. and McDougall, I. 2001. Superconductivity of Powder-In-Tube MgB_2 Wires. *Superconductor Science and Technology* 14:193.

Glowacki, B.A., Majoros, M., Vickers, M. and Zeimetz, B. 2002. Superconducting Properties of the Powder-in-Tube Cu–Mg–B and Ag–Mg–B Wires. *Physica C* 372: 1254.

Goldacker, W., Schlacter, S.I., Zimmer, S. and Reiner, H. 2001. High Transport Currents in Mechanically Reinforced MgB_2 Wires. *Superconductor Science and Technology* 14(9):787-793.

Grasso, G., Malagoli, A., Ferdeghini, C., Roncallo, S., Braccini, V. and Siri, A.C. 2001. Large Transport Critical Currents in Unsintered MgB_2 Superconducting Tapes. *INFM-Research Unit of Genova* 1-12.

Greenwood, N. N. 1973. Boron in J. C. Bailar (ed.): Comprehensive Inorganic Chemistry. *Pergamon Press* 1:680–689.

Hakola, Antti. 2008. Helsinki University of Technology. http://www.tkk.fi/.../prlaser/thesis/node3.html. (accessed March 23, 2008).

Harvard University. 2008. http://www.hoffman.physics.harvard.edu/researcSCintro.php. (accessed May 7, 2008).

Hascicek, Y.S., Aslanoğlu, Z. and Arda, L. 2004. Characterization of MgB_2 Conductors for Coil Development. *Adv.Cryo.Eng.* 50:541.

Higashikawa, K., Nakamura, T., Osamura, K., Takahashi, M. and Okada M. 2005. Switching Characteristics of MgB_2 Wires Subjected to Transient Application of Magnetic Field. *Physica C* 426-431:1261-1266.

Hinks, D.G., Jorgensen, J.D., Zheng, H., Short, S. 2002. Synthesis and Stoichiometry of MgB_2. *Physica C* 382:166.

Hishinuma, Y., Kikuchi, A. and Takeuchi, T. 2007. Superconducting Properties and Microstructure of MgB_2 Wires Synthesized with a Low-Temperature Diffusion Process. *Superconductor Science and Technology* 20:1178–1183.

Hyper Tech Research, Incorporation. 2008. Superconductors for Medical and Energy Products. http://www.hypertechresearch.com/page4.html. (accessed 2 May, 2008).

Institute of Experimental Physics. 2008. Tugraz University of Technology. http://www.iep.tugraz.at/.../index_eng.html. (accessed April 24, 2008).

Jiang, J., Senkowicz, B.J., Larbalestier, D.C. and Hellstrom, E.E. 2006. Influence of Boron Powder Purification on the Connectivity of Bulk MgB_2. *Superconductor Science and Technology* 19:L33-L36.

Jiang, C.H. and Kumakura, H. 2007. Stoichiometry Dependence of the Critical Current Density in Pure and Nano-SiC Doped MgB_2/Fe Tapes. *Physica C* 451:71-76.

Josephson, B.D. 1962. Possible New Effects in Superconductive Tunneling. *Physical Letters* 1:251-253.

Jung, C.U., Park, M.S., Kang, W.N., Kim, M.S., Lee, S.Y. and Lee, S.I. 2001. Temperature and Magnetic Field Dependent Resistivity of MgB_2 Sintered at High Temperature and High Pressure Condition. *Physica C* 353:162-166.

Kambara, M., Hari Babu, N., Sadki, E.S., Cooper, J.R., Minami, H., Cardwell, D.A., Campbell, A.M. and Inove, I.H. 2001. High Intergranular Critical Currents in Metallic MgB_2 Superconductor. *Superconductor Science and Technology* 14:L5-L7.

Kar, Y., Şen, N., and Demirbaş, A. 2006. Boron Minerals in Turkey, Their Application Areas and Importance for the Country's Economy. *Minerals & Energy-Raw Materials Report* 20:2-10.

Kılıç, A. M. 2004. *Importance of Boron Mine for Turkey and Place in the Future* Proceedings of the 2nd International Boron Symposium, 31-41.

Kılıç, A., Okur, S., Güçlü, N., Kölemen, U., Uzun, O., Ozyuzer, L. And Gencer, A. 2004. Structural and Low-Field Magnetic Characterization of Superconducting MgB_2 Wires. *Physica C* 415:51-56.

Kim, K.H.P., Choi, J.-H., Jung, C.U., Chowdhury, P., Lee, H.-S., Park, M.-S., Kim, H.J., Kim, J.Y., Du, Z., Choi, E.-M., Kim, M.-S., Kang, W.N., Lee, S.-I., Sung, G.Y., Lee, J.Y. 2002. Superconducting Properties of Well-Shaped MgB_2 Single Crystals. *Physical Review* 65:100510.

Kitaguchi, H., Nakane, T. and Kumakura, H. 2006. Fabrication of *ex-situ* MgB_2/Al Tapes and the Effects of In and SiC Addition. Preprint of the paper 3MJ04. *National Institute for Materials Science* (NIMS), Tsukuba, Japan.

Komori, K., Kawagishi, K., Takano, Y., Arisawa, S., Kumakura, H., Fukutomi, M., Togano, K. 2002. Approach for the Fabrication of MgB_2 Superconducting Tape with Large In-Field Transport Critical Current Density. *Applied Physics Letters* 81:1047.

Kováč, P., Hušek, I., Melišek, T., Grivel, J.C., Pachla, W., Štrbík,V., Diduszko, R., Homeyer, J. And Andersen, N.H. 2004. The Role of MgO Content in *ex-situ* MgB_2 Wires. *Superconductor Science and Technology* 17:L41-L46.

Kováč, P., Hušek, I., Melišek, T., Martínez, E. and Dhalle, M. 2006. Properties of Doped *ex* and *in situ* MgB_2 Multi-filament Superconductors. *Superconductor Science and Technology* 19:1076–1082.

Larbalestier, D.C., Cooley, L.D., Rikel, M.O., Polyanskii, A.A., Jiang, J., Patnaik, S., Cai, X.Y., Feldmann, D.M., Gurevich, A., Squitieri, A.A., Naus, M.T., Eom, C.B., Hellstrom, E.E., Cava, R.J., Regan, K.A., Rogado, N., Hayward, M.A., He, T., Slusky, J.S., Khalifah, P., Inumaru, K., and Haas, M. 2001. Strongly Linked Current Flow in Polycrystalline Forms of the Superconductor MgB_2. *Nature* 410:186.

Li, X.H., Du, X.H., Qiu, M., Ma, Y.W. and Xiao, L.Y. Flukiger, R., Suo, H.L., Musolino, N., Beneduce, C., Toulemonde, P., Lezza, P. 2003. Superconducting Properties of MgB_2 Tapes and Wires. *Physica C* 385:286-305.

London, Fritz. and London, Heinz. 1935. The Electromagnetic Equations of the Supraconductor. *Proc. Roy. Soc.* A149:71-88.

Machi, T., Shimura, S., Koshizuka, N. and Murakami, M. 2003. Fabrication of MgB_2 Superconducting Wire by *in situ* PIT Method. *Physica C* 392-396:1039-1042.

Maeda, H., Tanaka, Y., Fukutomi, M., and Asano, T. 1988. A New High-Tc Oxide Superconductor without a Rare Earth Element. *Jpn.J.Appl.Phys.* 27:L209-L210.

Mark, Herman F. and John J. McKetta JR, eds. 2001. *Boron, Elemental*. New York: Kirk-Othmer Encyclopedia of Chemical Technology, *Interscience Publisher John Wiley and Sons, Incorporation.*

Meissner, W. and Ochsenfeld R. 1933. Ein neuer Effekt bei Eintritt der supraleitfähigkeit. *Naturwissenschaften* 21: 787-788.

Microwave Encylopedia. 2006. http://www.microwaves101.com/encylopedia/conductivity.cfm. (accessed April 29, 2008)

Moon, S.H., Yun, J.H., Lee, H.N., Kye, J.I., Kim, H.G., Chung, W. and Oh, B. 2001. High Critical Current Densities in Superconducting MgB_2 Thin Films. *Applied Physics Letters* 79:2429.

Mudgel, M., Awana, V.P.S., Kishan, H. and Bhalla, G.L. 2008. Significant Improvement of Flux Pinning and Irreversibility Field in Nano-Carbon-Doped MgB_2 Superconductor. *Solid State Communications* in press.

Musenich, R., Greco, M., Razeti, M. and Tavilla, G. 2007. Electrical Characterization of a Multi-Strand MgB_2 Cable. *Superconductor Science and Technology* 20:235-238.

Musenich, R., Fabbricatore, P., Fanculli, C., Ferdeghini, C., Grasso, M., Greco, M., Malagoli, A., Marabotto, R., Modica, M., Siri, A. and Tumino, A. 2004. *IEEE Transactions on Applied Superconductivity* 14:2.

Nagamatsu, J., Nakagawa, T., Muranaka, Zenitani Y., and Akimitsu, J. 2001. Superconductivity at 39 K in Magnesium Diboride. *Nature* 410(6824):63-64.

National Boron Research Institute. 2008. http://www.boren.gov.tr (accessed February 13, 2008).

Narayana, Sh. S. 1954. The Institution of Electronics and Telecommunication Engineers (IETE) e-Learning & Networks. http://iete-elan.ac.in/.../Dec2004/Sol-D04-1-D2K4.htm. (accessed May 14, 2008).

Okur, S., Kalkanci, M., Yavas, M., Egilmez, M. and Ozyuzer, L. 2005. Microstructural and Electronic Characterization of Ti and Mg Doped Copper-Clad MgB_2 Superconducting Wires. *Journal of Optoelectronics and Advanced Materials* 7:411-415.

Onnes, Kamerlingh. 1911. The Superconductivity of Mercury. Comm. Phys. Lab. Univ. Leiden 122-124:1226.

Özkan, S. 2007. Production of SiC Particle Reinforced Aluminium Matrix Based Composites by Mechanical Alloy Method and Investigation of Their Wear Behavior. *Gazi University thesis of M.Sc.*

Pachla, W., Moravski, A., Kováč, P., Hušek, I., Mazur, A., Lada, T., Diduszko, R., Melišek, T. and Štrbík,V. 2006. Properties of Hydrostatically Extruded *in situ* MgB_2Wires Doped with SiC. *Superconductor Science and Technology* 19:1-8.

Pradhan, A.K., Shi, Z.X., Tokunaga, M., Tamegai, T., Takano, Y., Togano, K., Kito, H., Ihara, H. 2001. Electrical Transport and Anisotropic Superconducting Properties in Single Crystalline and Dense Polycrystalline MgB_2. *Physical Review Letters* 64:212509.

Ribeiro, R.A., Bud`ko, S.L., Petrovic, C., Canfield, P.C. 2002. Effects of Stoichiometry, Purity, Etching and Distilling on Resistance of MgB_2 Pellets and Wire Segments. *Physica C* 382: 194.

Ribeiro, R.A., Bud`ko, S.L., Petrovic, C. and Canfield, P.C. 2003. Carbon Doping of Superconducting Magnesium Diboride. *Physica C* 384:227-236.

Ribeiro, R.A., Bud`ko, S.L., Petrovic, C. and Canfield, P.C. 2003. Effects of Boron Purity, Mg Stoichiometry and Carbon Substitution on Properties of Polycrystalline MgB_2. *Physica C* 385:16-23.

Salama, K. and Fang, H. 2007. Method of Manufacturing Fe-Sheathed MgB_2 Wires and Solenoids. *U.S. Patent* US 7,213,325 B2.

Serquis, A., Civale, L., Hammon, D.L., Coulter, J.Y., Liao, X.Z., Zhu, Y.T., Peterson, D.E. and Mueller, F.M. 2003. Microstructure and High Critical Current of Powder in Tube MgB_2. *Applied Physics Letters* 82:1754.

Serquis, A., Civale, L. and Hammon, L. 2003. Hot Isostatic Pressing of Powder in Tube MgB_2 Wires. *Applied Physics Letters* 82:2847.

Serquis A., Civale L., Coulter J. Y., Hammon D. L., Liao X. Z., Zhu Y. T., Peterson D. E., Mueller F. M., Nesterenko V. F. and Indrakanti S. S. 2004. Large Field Generation with Hot Isostatically Pressed Powder-in-Tube MgB_2 coil at 25 K. *Rapid Communication* 0404052:3-23.

Serquis, A., Civale L., Hammon, D.L., Serrano G., and Nesterenko V. F. 2005. Optimization of Critical Currents in MgB_2 Wires and Coils. *IEEE Transactions On Applied Superconductivity* 15:3188-3191.

Sheng, Z.Z., and Hermann, A.M. 90 K *Tl-Ba-Cu-O* and 120 K *Tl-Ca-Ba-Cu-O* Bulk Superconductors, Proc. In 1988 World Congress on Superconductivity. Singapore: World Scientific.

Shi, Q.Z., Liu, Y.C., Zhao, Q. and Ma, Z.Q. 2007. Phase Formation process of Bulk MgB_2 Analyzed by Differential Thermal Analysis during Sintering. Journal of Alloys and Compounds 458:553-557.

Shimura, S., Machi, T., Murakami, M., Koshizuka, N., Mochizuki, K., Ishikawa, I. And Shibata, N. 2004. Copper Sheath MgB_2 Wires Fabricated by an *in situ* PIT Method. *Physica C* 412-414:1179-1183.

Sivrikaya, H. and Saraçbaşı, A. 2004. *Evaluation Boron Mine in Wood Protection Industry.* Eskişehir: Proceedings of the 2nd International Boron Symposium, 366.

Smith, Robert A. 2002. *Boric Oxide, Boric Acid ,and Borates-Uses.* Germany: Ullmann's Encyclopedia of Industrial Chemistry, Sixth Edition.

Soltanian, S., Horvat, J., Wang, X. L., Horvat, J., Li, A.H., Liu, H.K. and Dou, S.X. 2002. Improvement of Critical Current Density in the Cu/MgB_2 and Ag/MgB_2 Superconducting Wires Using the Fast Formation Method. *Superconductor Science and Technology* 382:187-193.

Soltanian, S., Horvat, J., Wang, X. L., Tomsic, M. and Dou, S.X. 2003. Transport Critical Current of Solenoidal MgB_2/Cu Coils Fabricated Using a Wind-reaction *in situ* technique. *Superconductor Science and Technology* 16:L4-L6.

Soltanian, S. 2004. Development of Superconducting Magnesium Diboride Conductors. *University of Wollongong thesis of PhD.*

Sonoma State University. 2008. http://www.nbsp.sonoma.edu/resources/teachers_materials/physical_01/electricity/sld028.htm. (accessed April 30, 2008).

Stenvall, A., Hiltunen, I., Korpela, A., Lehtonen, J., Mikkonen, R., Viljamaa, J. and Grasso, G. 2007. A Checklist for Designers of Cryogen-Free Coils. *Superconductor Science and Technology 20:386-391.*

Sumption, M.D., Bhatia, M., Rindfleisch, M., Phillips, J., Tomsic, M., and Collings, E.W. 2004. MgB_2/Cu Racetrack Coil: Winding and Transport Testing. *Superconductor Science and Technology 1-20.*

Sumption, M.D., Bhatia, M., Rindfleisch, M., Tomsic, M. and Collings, E.W. 2005. Transport and Magnetic Jc of MgB_2 Strands and Small Helical Coils. *Applied Physics Letters* 86:102501.

Sumption, M.D., Bhatia, M., Rindfleisch, M., Tomsic, M., Soltanian, S., Dou, S.X. and Collings, E.W. 2005. Large Upper Critical Field and Irreversibility Field in MgB_2 Wires with SiC Additions. *Applied Physics Letters* 86:092507.

Suo, H.L., Lezza, P., Uglietti, D., Beneduce, C., Abuacherli, V., Flukiger, R. 2002. Transport Critical Current Densities and n Factors in Mono-and Multifilamentary MgB_2/Fe Tapes and Wires Using Fine Powders. *Applied Superconductivity* in press.

Susner, M.A., Sumption, M.D., Bhatia, M., Peng, X., Tomsic, M.J., Rindfleisch, M.A. and Collings, E.W. 2007. Influence of Mg/B Ratio and SiC Doping on Microstructure and High Field Transport Jc in MgB_2 Strands. *Physica C* 456:180-187.

Sümer, G. 2004. *Boron Compounds*. Eskişehir: Proceedings of the 2nd International Boron Symposium, 157-163.

Takano, K., Takeya, H., Fujii, H., Kumakura, H., Hatano, T., Togano, K. 2001. Superconducting Properties of MgB_2 Bulk Materials Prepared by High-Pressure Sintering. *Applied Physical Letters* 78:2914.

Tanaka, K., Okada, M., Kumakura, H., Kitaguchi, H., Togano K. 2002. Fabrication and Transport Properties of MgB_2 Wire and Coil. *Physica C* 382:203-206.

The University of Oxford. 2007. http://www.ncl.ox.ac.uk/.../lecture2/elemtal.html (accessed March 20, 2007).

Tomsic, M., Rindfleisch, M., Yue, J., McFadden, K. and Philips, J. 2007. Overview of MgB_2 Superconductor Applications. *International Journal of Applied Ceramic Technology* 4(3):250-259.

Tomsic, M., Rindfleisch, M., Yue, J., McFadden, K., Doll, D., Philips, J., Sumption, M.D., Bhatia, M., Bohnenstiehl, S. and Collings, E.W. 2007. Development of Magnesium Diboride (MgB_2) Wires and Magnets Using in situ Strand Fabrication Method. *Physica C 456:203-208*.

Vinod, K., Varghese, N., Abhilash Kumara, R.G., Syamaprasad, U., Roy, S.B. 2007. Influence of Mg Particle Size on the Reactivity and Superconducting Properties of *in situ* MgB_2. *Journal of Alloys and Compounds* in press.

Vinod, K., Abhilash Kumara, R.G. and Syamaprasad, U. 2007. Prospects for MgB_2 Superconductors for Magnet Application. *Superconductor Science and Technology* 20:R1-R13.

Wang X.L., Soltanian, S., Horvat, J., Liu, A. H., Qin, M.J., Liu, H.K. and Dou, S.X. 2001. Very Fast Formation of Superconducting MgB_2/Fe Wires with High J_c, *Physica C* 361:149-155.

Wang, J., Bugoslavsky, Y., Berenov, A., Cowey, L., Caplin, A.D., Cohen, L.F., MacManus, Driscoll, J.L., Cooley, L.D., Song, X., Larbalestier, D.C. 2002. High Critical Current Density and Improved Irreversibility Field in Bulk MgB_2 Made by a Scaleable, Nanoparticle Addition Route. *Applied Physics Letters* 81:2026.

Wesche, Rainer. 1998. *High-Temperature Superconductors: Materials, Properties, and Applications.* Switzerland: Kluwer Academic Publishers.

Wu, M.K., Ashburn J.R., Torng, C.J., Hor, P.H., Meng, R.L., Gao, L., Huang, Z.J., Wang and Chu, C.W. 1987. Superconductivity at 93K in a Mixed-Phase Yb-Ba-Cu-O Compound System at Ambient Pressure. *Physical Review Letters* 58(9):908-910.

Xiang, J.Y., Zheng, D.N., Li, J.Q., Li, S.L., Wen, H.H. and Zhao, Z.X. 2003. Effects of Al Doping on the Superconducting and Structural Properties of MgB_2. *Physica C* 386:611.

Xiao, H., Peng, W., Song, W.H., Ma, R.C., Zhang, L., Du, J.J. and Sun, Y.P. 2003. Influence of Mg Deficiency on the Properties of MgB_2. *Physica C* 386:648-652.

Xu, H.L., Feng, Y., Xu, Z., Li, C.S., Yan, G., Mossang, E., Sulpice, A. 2005. Effect of Sintering Temperature on Properties of MgB_2 Wire Sheathed by Low Carbon Steel Tube. *Physica C* 419:94-100.

Yamamoto, K., Osamura, K., Balamurugan, S., Nakamura, T., Hoshino, T. and Muta, I. 2003. Mechanical and Superconducting Properties of PIT-Processed MgB_2. Wire after Heat Treatment. *Superconductor Science and Technology* 16:1052-1058.

Yamamoto, A., Shimoyama, J., Kishio, K. and Matsushita, T. 2007. Limiting Factors of Normal-State Conductivity in Superconducting: An Application of Mean-Field Theory MgB_2. *Superconductor Science and Technology* 16:L4-L6.

Yan, G., Fu, B.Q., Feng, Y., Liu, C.F., Ji, P., Wu, X.Z., Zhou, L., Cao, L.Z., Ruan, K.Q. and Li, X.G. 2003. Preparation and Transport *Jc*(B) Properties of Fe-Clad MgB_2 Wires. *Physica C* 386:607-610.

Yan, S.C., Yan, G., Liu, C.F., Lu, Y.F. and Zhou, L. 2007. Experimental Study on Phase Transformation between MgB_2 and MgB_4. *Journal of the American Ceramic Society* 90:2184-2188.

Yavaş, M. 2004. Fabrication and Characterization of MgB_2 Powders and Cu-Clad MgB_2 Wires. *İzmir Institute of Technology thesis of M.Sc.*

Yavaş, M., Okur, S., Eğilmez, M., Kalkanci, M. and Özyüzer, L., 2005. Fabrication of Superconducting MgB_2 from Boric Acid (H_3BO_3) and its Microstructural and Electrical Characterization. *Journal of Optoelectronics and Advanced Materials* 7:407-411.

Yen, L., Majoros, M., Campbell, A.M., Coombs, T., Astill, D., Harrison, S., Husband, M., Rindfleisch, M. and Tomsic, M. 2007. Experimental Studies of the Quench Behaviour of MgB_2 Superconducting Wires for Fault Current Limiter Applications. *Superconductor Science and Technology* 20:621-628.

Yıldıran, H. and Güler. S.D. 2006. The Production of Elemental Boron (Amorphous and Crystallic) in a Simple and Economical Method. *Patent International Publication* Number WO2006135350.

Yıldırım, T. and Gülseren, O. 2002. A Simple Theory of 40 K Superconductivity in MgB_2: First Principles Calculations of Tc, its Dependence on Boron Mass and Pressure. *Journal of Physics and Chemistry of Solids* 63:2201-2206.

Zhao, Y., Feng, Y., Cheng, Y., Zhou, L., Wu, Y., Machi, T., Fudamoto, Y., Koshizuka, N. and Murakami, M. 2001. High Critical Current Density of MgB_2 Bulk Superconductor Doped with Ti and Sintered at Ambient Pressure. *Applied Physics Letters* 79:1514.

Zhao, Y., Feng, Y., Huang, D.X., Machi, T., Cheng, C.H., Nakao, K., Chikumoto, N., Fudamoto, Y., Koshizuka, N., Murakami, M. 2002. Doping Effect of Zr and Ti on the Critical Current Density of MgB_2 Bulk Superconductors Prepared Under Ambient Pressure. *Physica C* 378-381:122.

Zhao, Y., Huang, D.X., Feng, Y., Cheng, C.H., Machi, T., Koshizuka, N., Murakami, M. 2002. Nanoparticle Structure of MgB_2 With Ultrathin TiB_2 Grain Boundaries *Applied Physics Letters* 80:1640.

Zhao, Q., Liu, Y., Shi, Q., Ma, Z. And Gao, Z. 2008. Characteristic and Synthesis Mechanism of MgB_2 Nanoparticles in Solid-State Reactive Sintering. *Journal of Alloys and Compounds* in press.